Local B-modes from Inflation and Defects

Benasque 2010
Modern Cosmology
Centre for Science "Pedro Pascual"

Juan García-Bellido
Inst. Física Teórica UAM
19th August 2010

Outline

Primordial Gravitational Waves from preheating

- Hybrid Inflation (tachyonic preheating)
- Abelian-Higgs Model (cosmic strings+fields)
- Detection with laser interferometers
- Anisotropic maps of PGW background

PGW from global phase transitions after Inflation

- Self ordering of Goldstone modes
- Scale invariant spectrum subhorizon scales
- Detection in B-mode Polarization of CMB

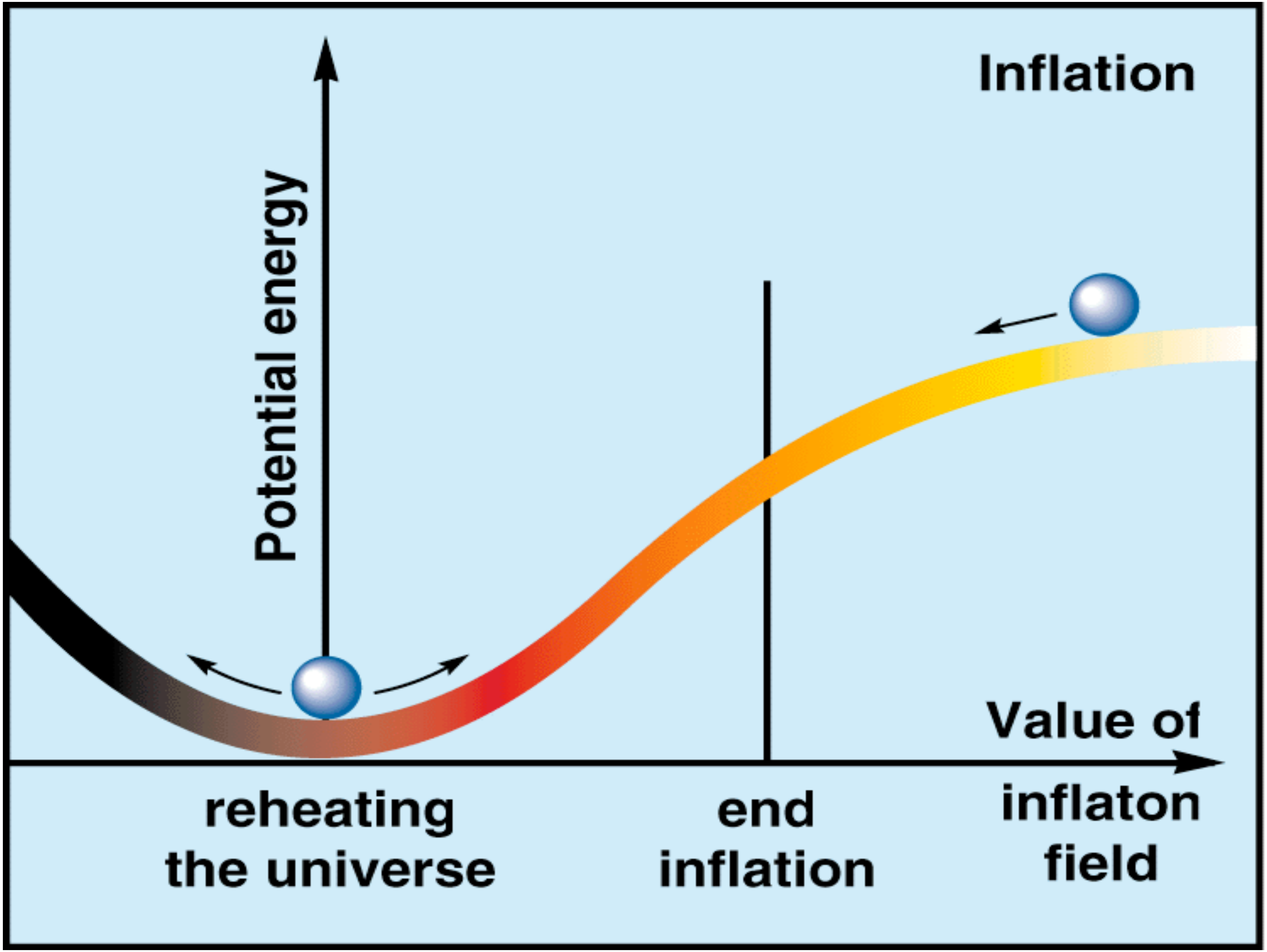
Inflation
Potential energy
Value of inflaton field
reheating the universe
end inflation

Preheating

Very rich phenomenology after inflation

- Non-thermal production of particles (CDM)
- Production of topological defects
- EW baryogenesis & leptogenesis
- Production of gravitational waves
- Production of primordial magnetic fields
- etc.

Hybrid preheating

JGB, Linde	PRD57, 6075 (1998)
Felder, JGB, Kofman, Linde, Tkachev	PRL87, 011601 (2001) PRD64, 123517 (2001)
JGB, García-Perez, González-Arroyo	PRD67, 103501 (2003) PRD69, 023504 (2004)

Tachyonic preheating

Spinodal growth of long wave Higgs modes

- At the end of Hybrid Inflation
- Higgs couples to gauge fields
- Strong production of fermions

The Abelian Higgs-Inflaton model

$$L = -\frac{1}{4} F^{a}_{\mu\nu} F^{\mu\nu}_{a} + Tr[(D_\mu \Phi)^+ D^\mu \Phi] + \frac{1}{2}(\partial_\mu \chi)^2 - V(\Phi, \chi)$$

$$D_\mu = \partial_\mu - ieA_\mu$$

$$F_{\mu\nu} = \partial_\mu A_\nu - \partial_\nu A_\mu$$

$$Tr[\Phi^+ \Phi] = \frac{1}{2}(\phi^a \phi_a) \equiv \frac{1}{2}\phi^2$$

$$V(\phi, \chi) = \frac{\lambda}{4}(\phi^2 - v^2)^2 + \frac{g^2}{2}\phi^2 \chi^2 + \frac{1}{2} m^2 \chi^2$$

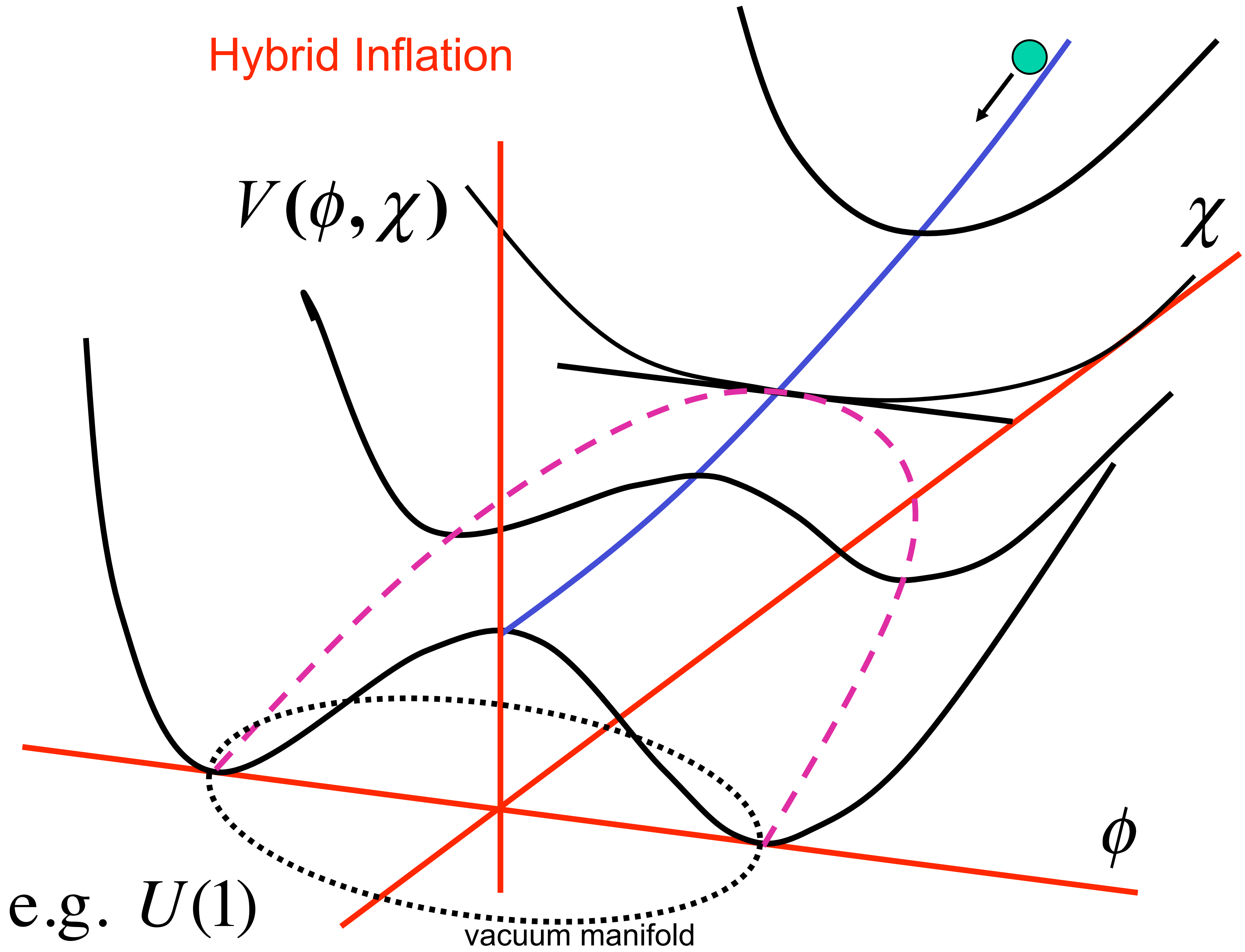
Hybrid Inflation
V(φ, χ)
χ
φ
e.g. U(1)
vacuum manifold

Lattice Simulations

Quantum averages = Ensemble averages

Initial conditions: Highly occupied modes

$$\left|0,\tau\right\rangle = U\left|0,\tau_0\right\rangle \;\Rightarrow\; \Psi_0(\tau) = \frac{1}{\sqrt{\pi}\,|f_k|} e^{-\Omega_k(\tau)|y_k^0|^2}$$

Rayleigh distribution: Gaussian random field

$$P_\Psi(|\phi_k|)d|\phi_k|d\theta_k = e^{-\frac{|\phi_k|^2}{|f_k|^2}} \frac{d|\phi_k|^2}{|f_k|^2}\frac{d\theta_k}{2\pi}$$

High peaks of Higgs field

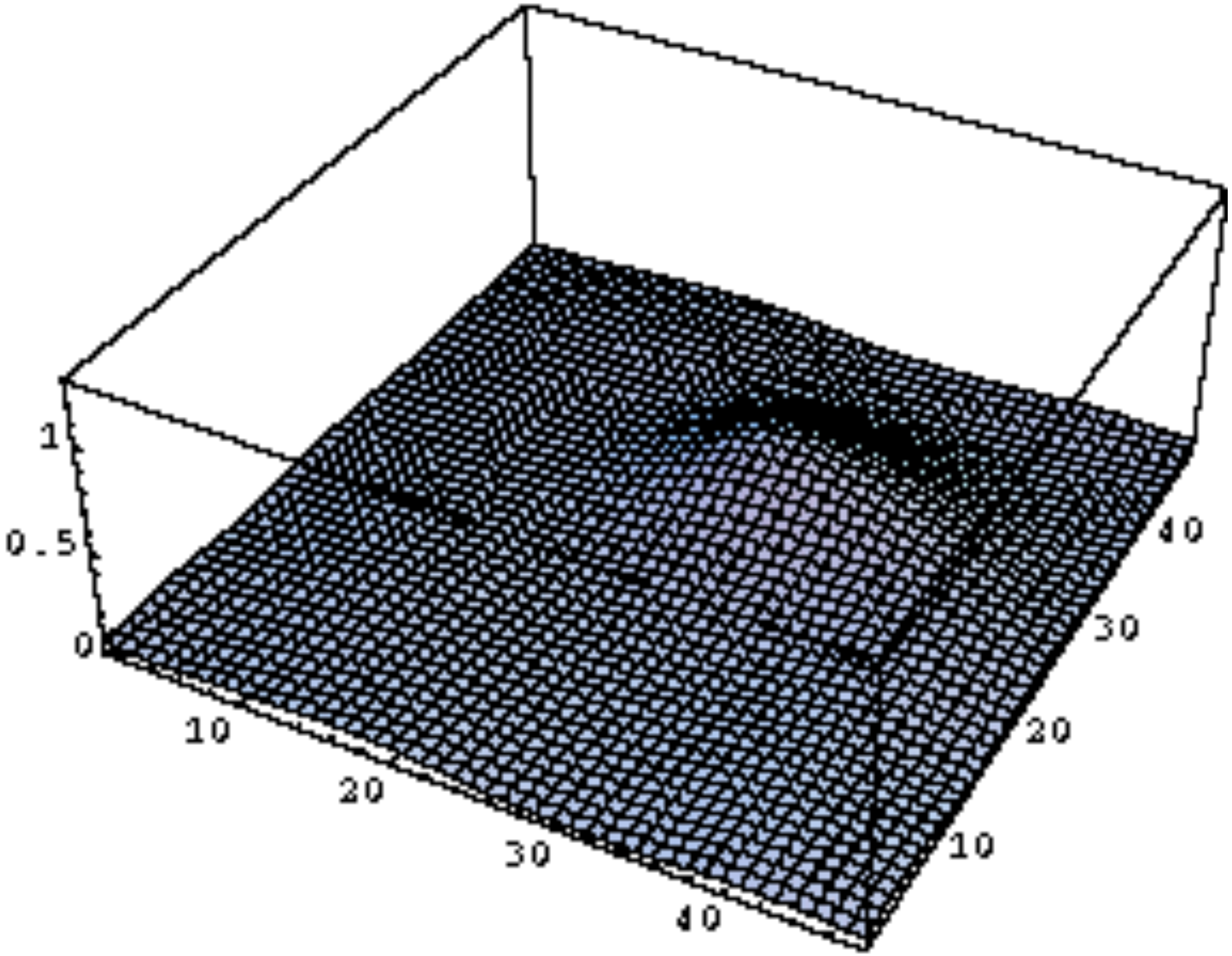

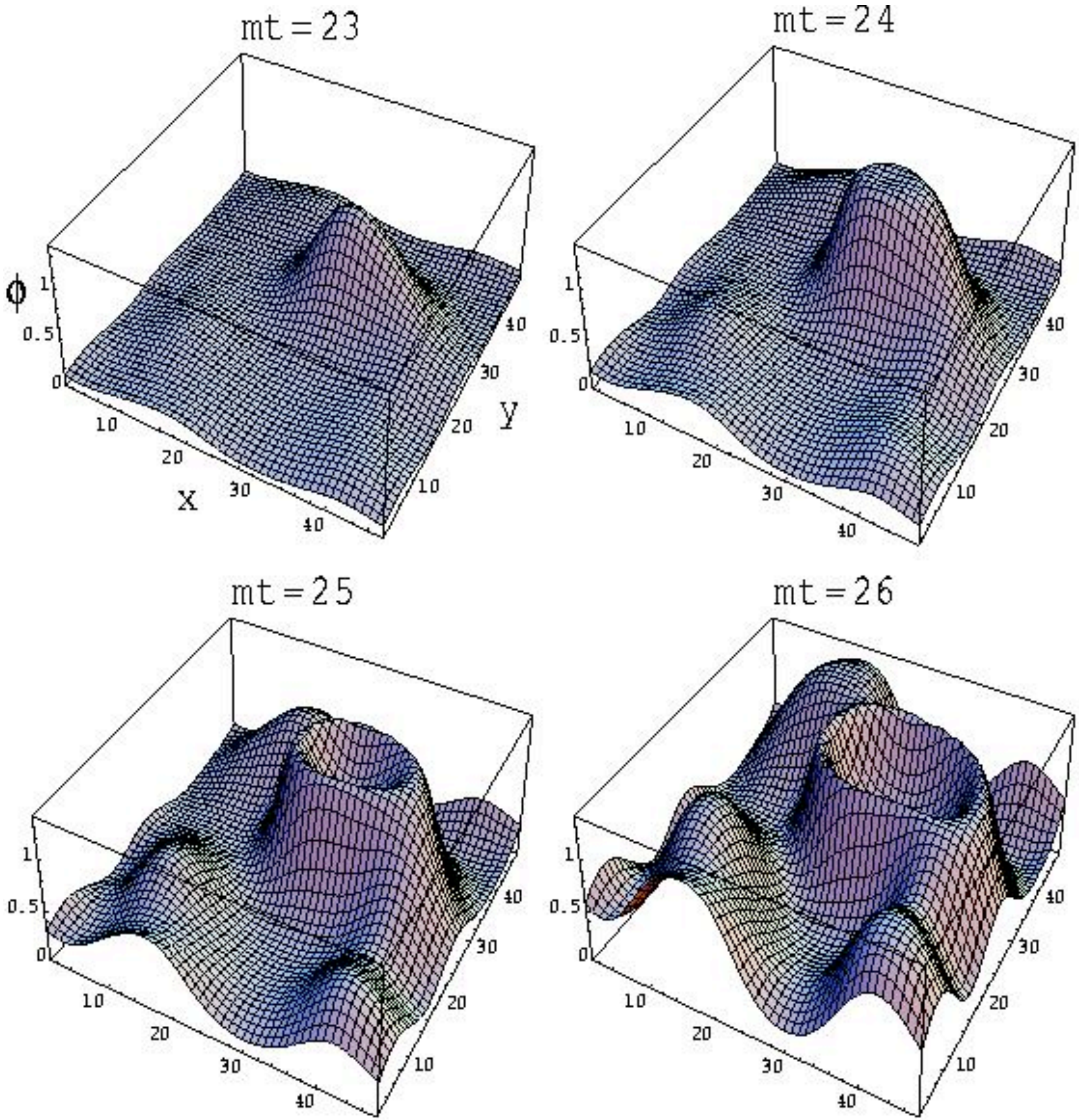

mt = 23
mt = 24
mt = 25
mt = 26
ϕ
x
y
0
0.5
1
10
20
30
40

Formation of Higgs bubbles

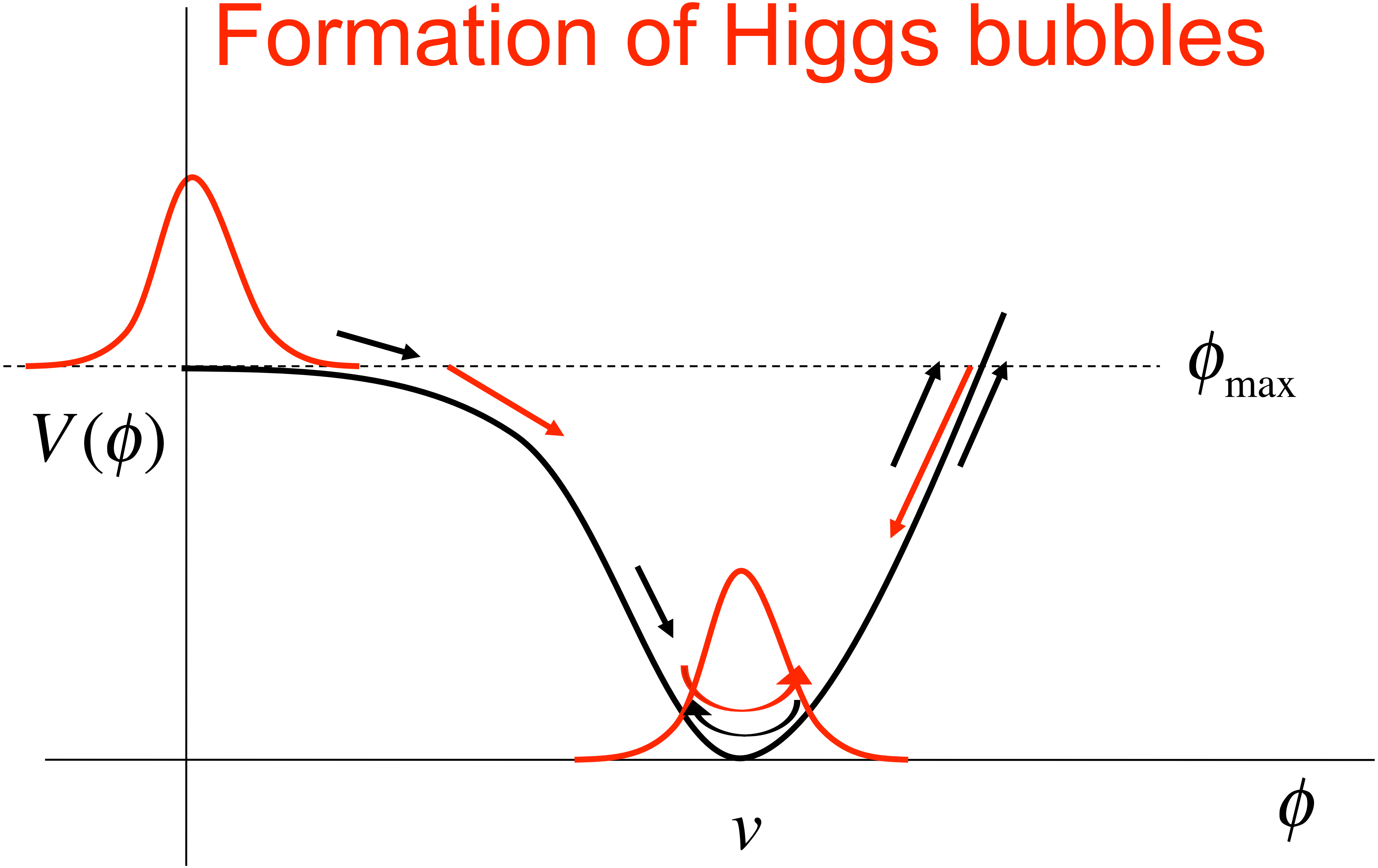

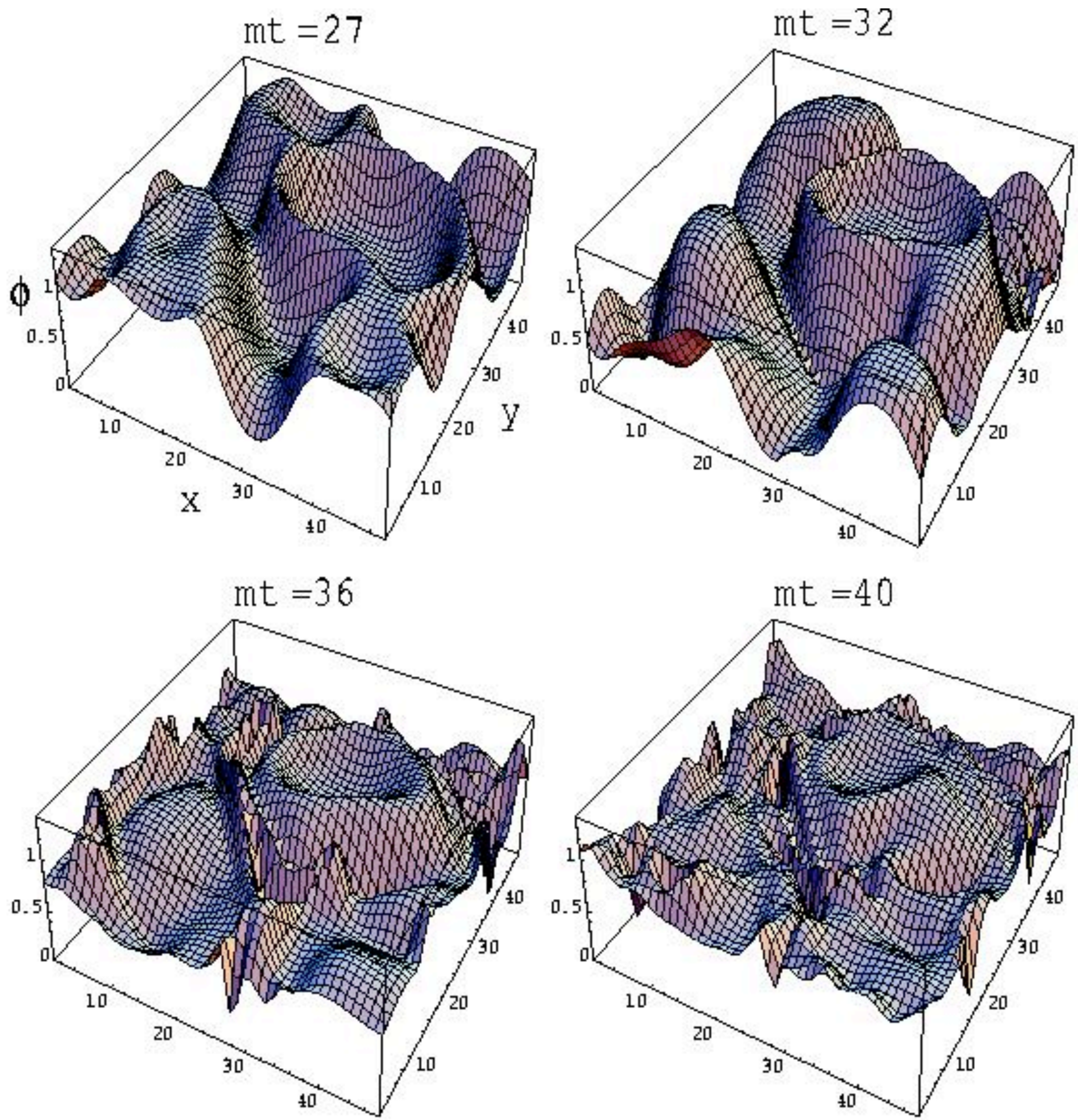
mt =27
mt =32
mt =36
mt =40
φ
x
y
0
0.5
1
10
20
30
40

Histogram of Re Φ and Im Φ

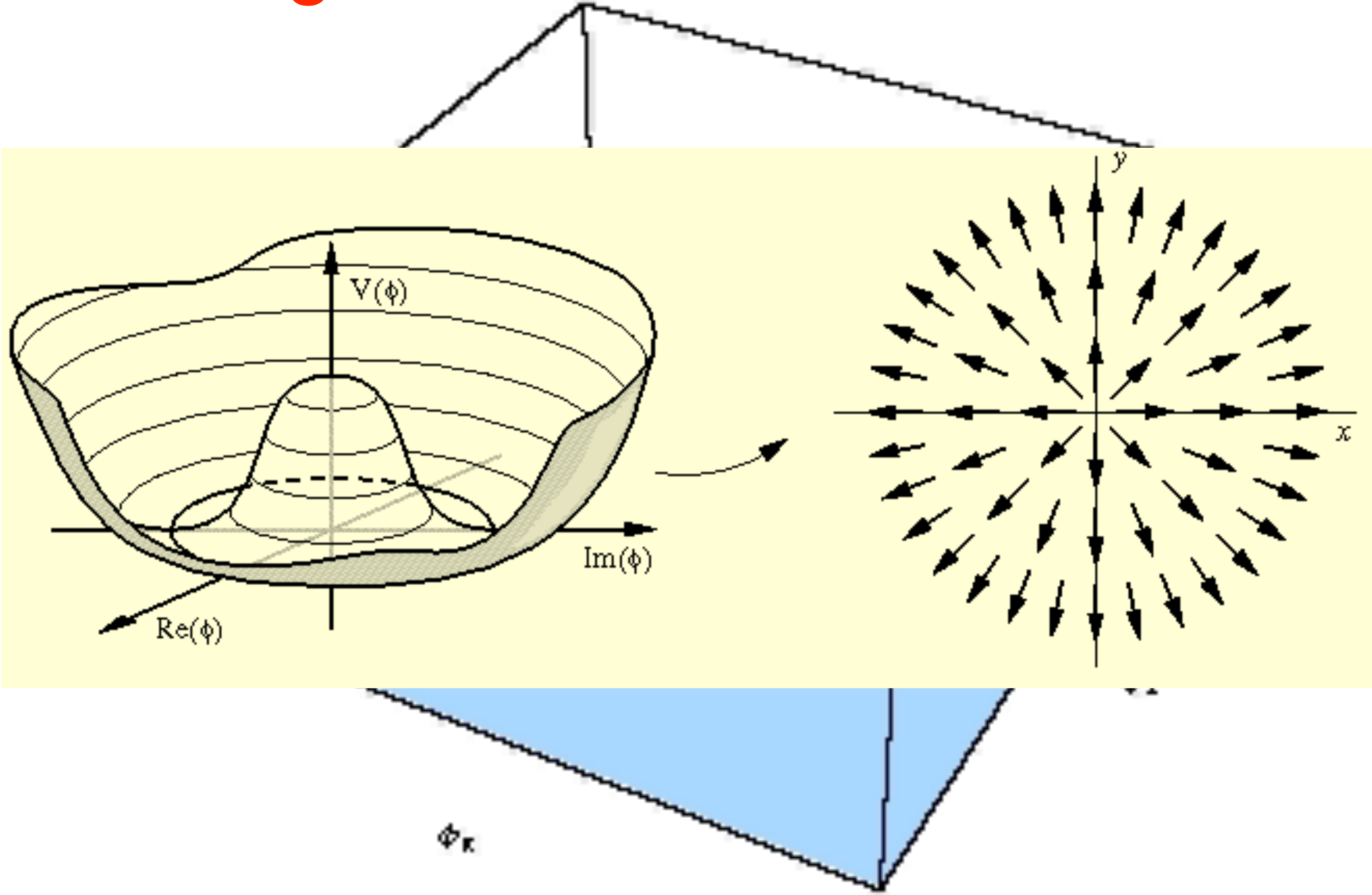

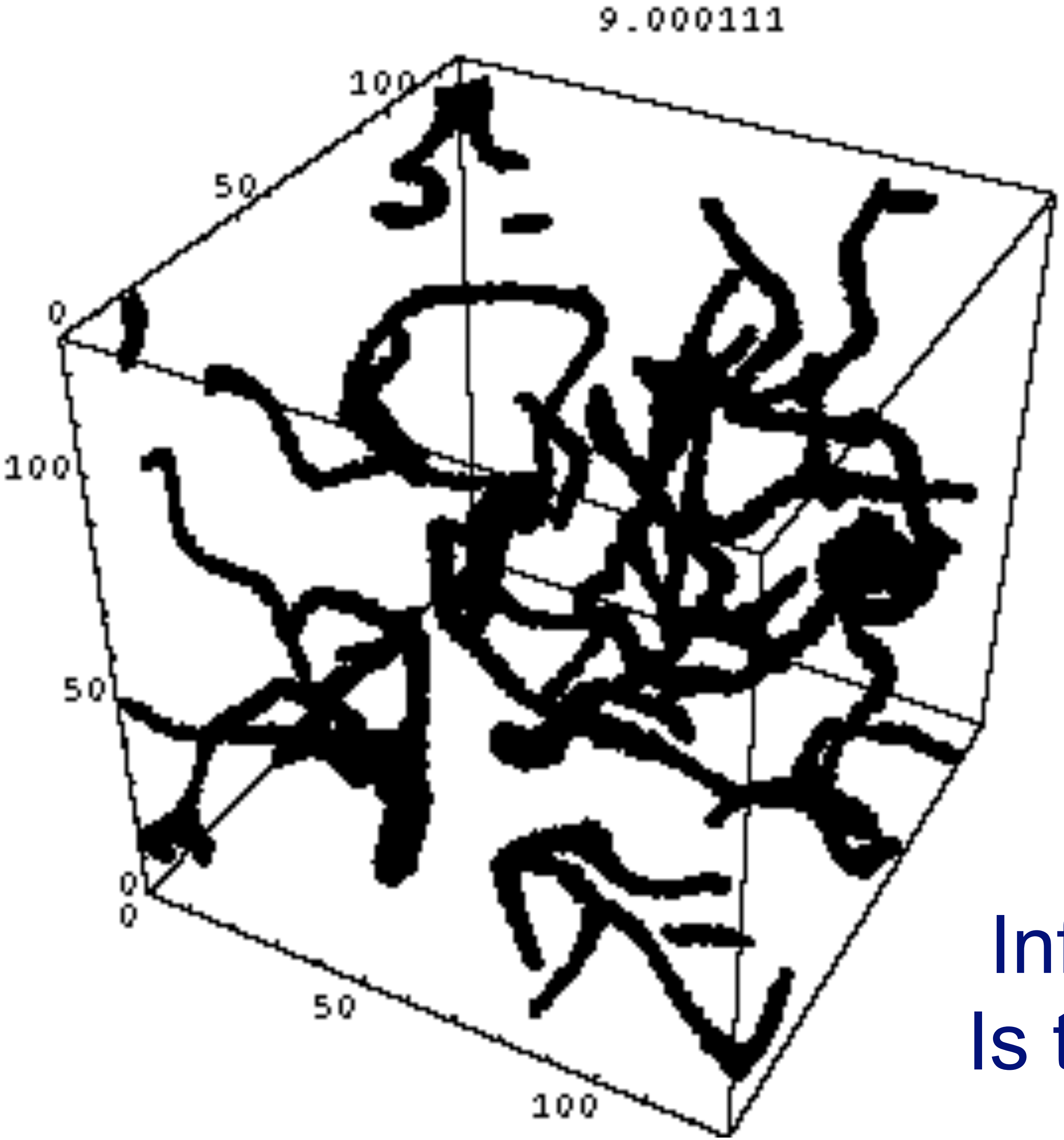

$\chi \in U(1)$

String production @ end inflation

How many Infinite strings? Is there scaling?

Stochastic background GW from preheating

Khlebnikov+Tkachev	PRD 56, 653 (1997)
JGB	arXiv:hep-ph/9804205
+Daniel G. Figueroa	PRL 98, 061302 (2007)
+Alfonso Sastre	PRD 77, 043517 (2008)
Easther et al.	PRL 99, 221301 (2007)
Price et al.	PRD 78, 063541 (2008)
Dufaux et al.	JCAP 0903, 001 (2009)

Time evolution after inflation

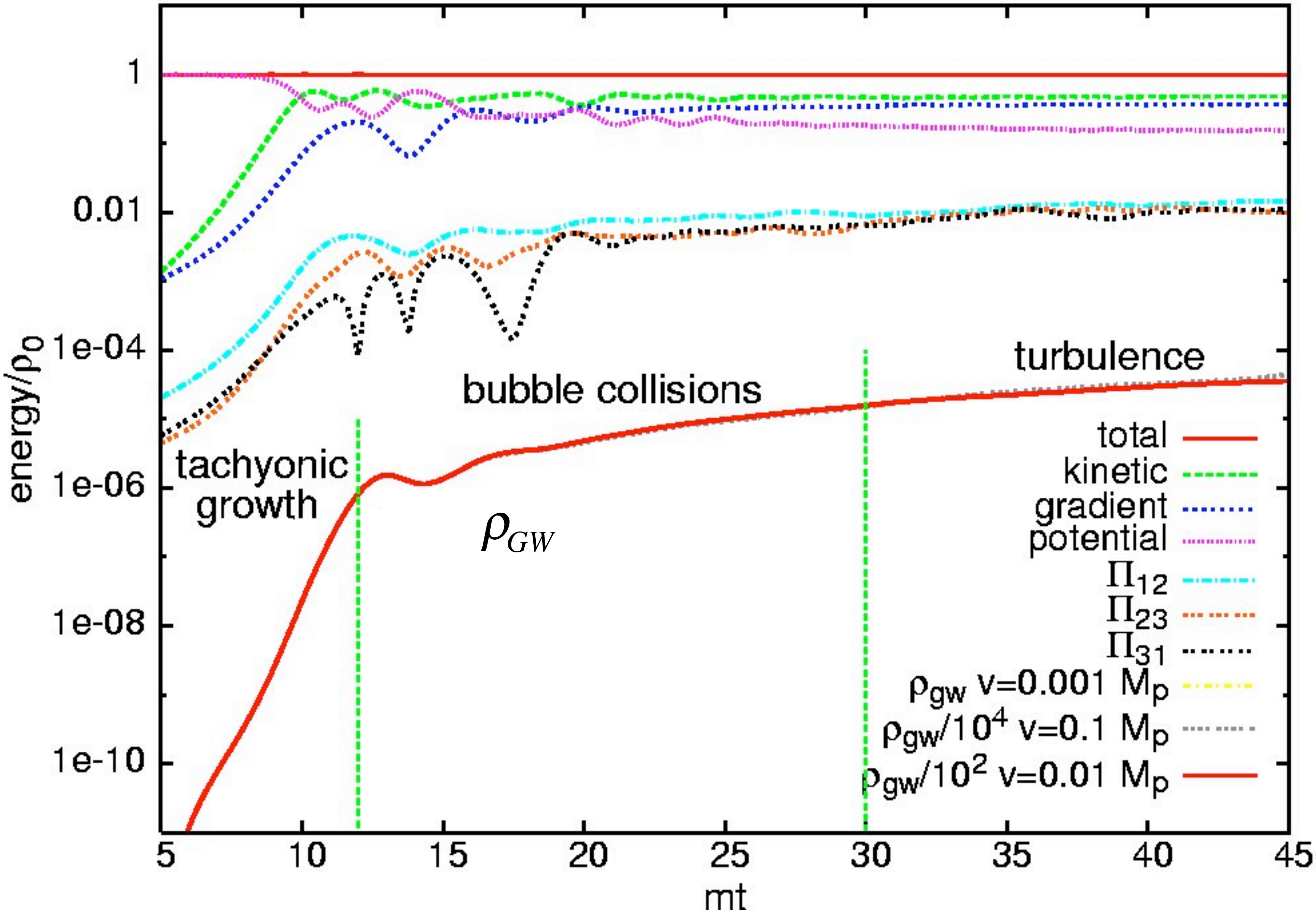

Gravitational Wave detectors in the world

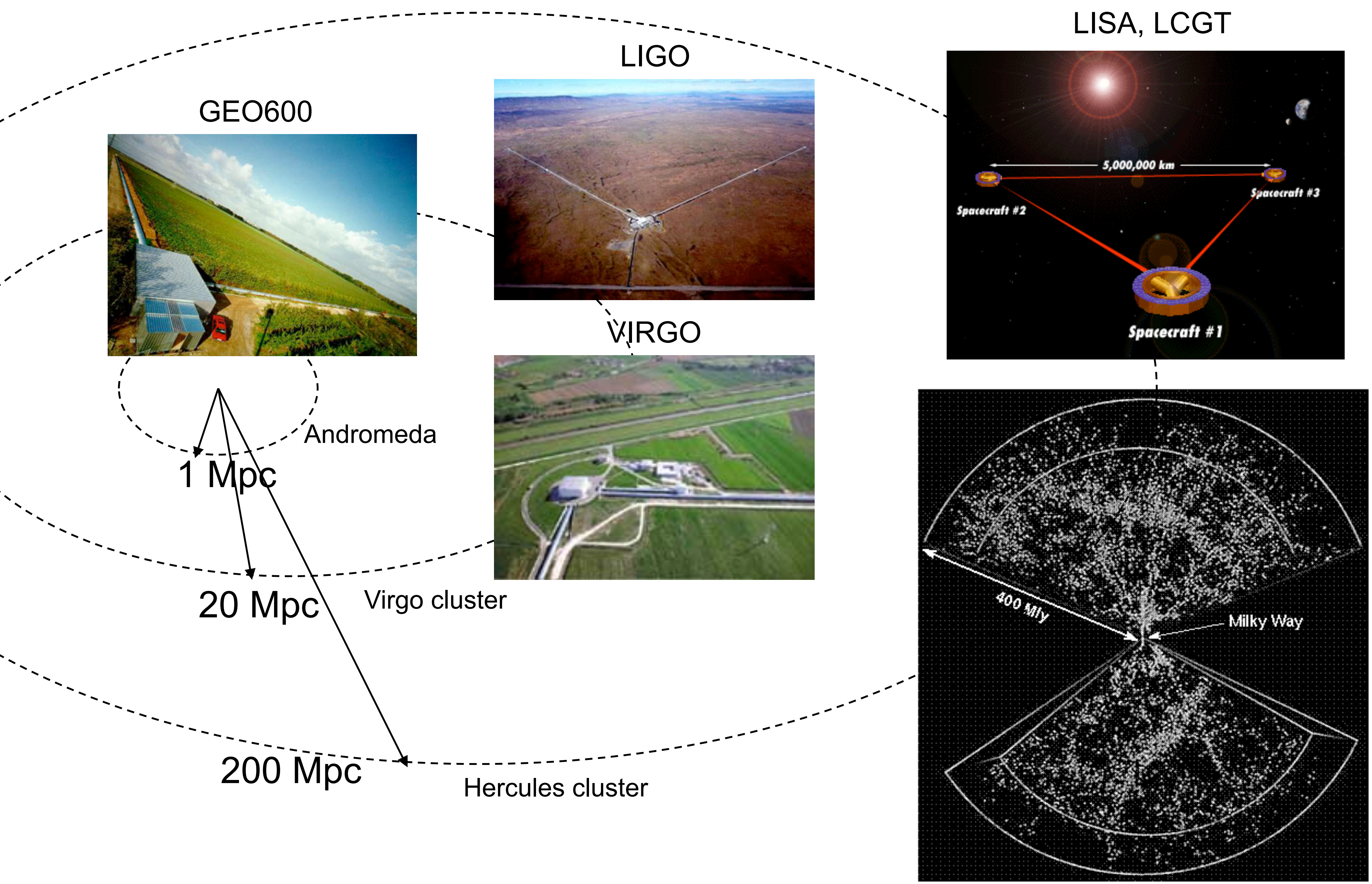

Backgrounds, Bounds & Sensitivity

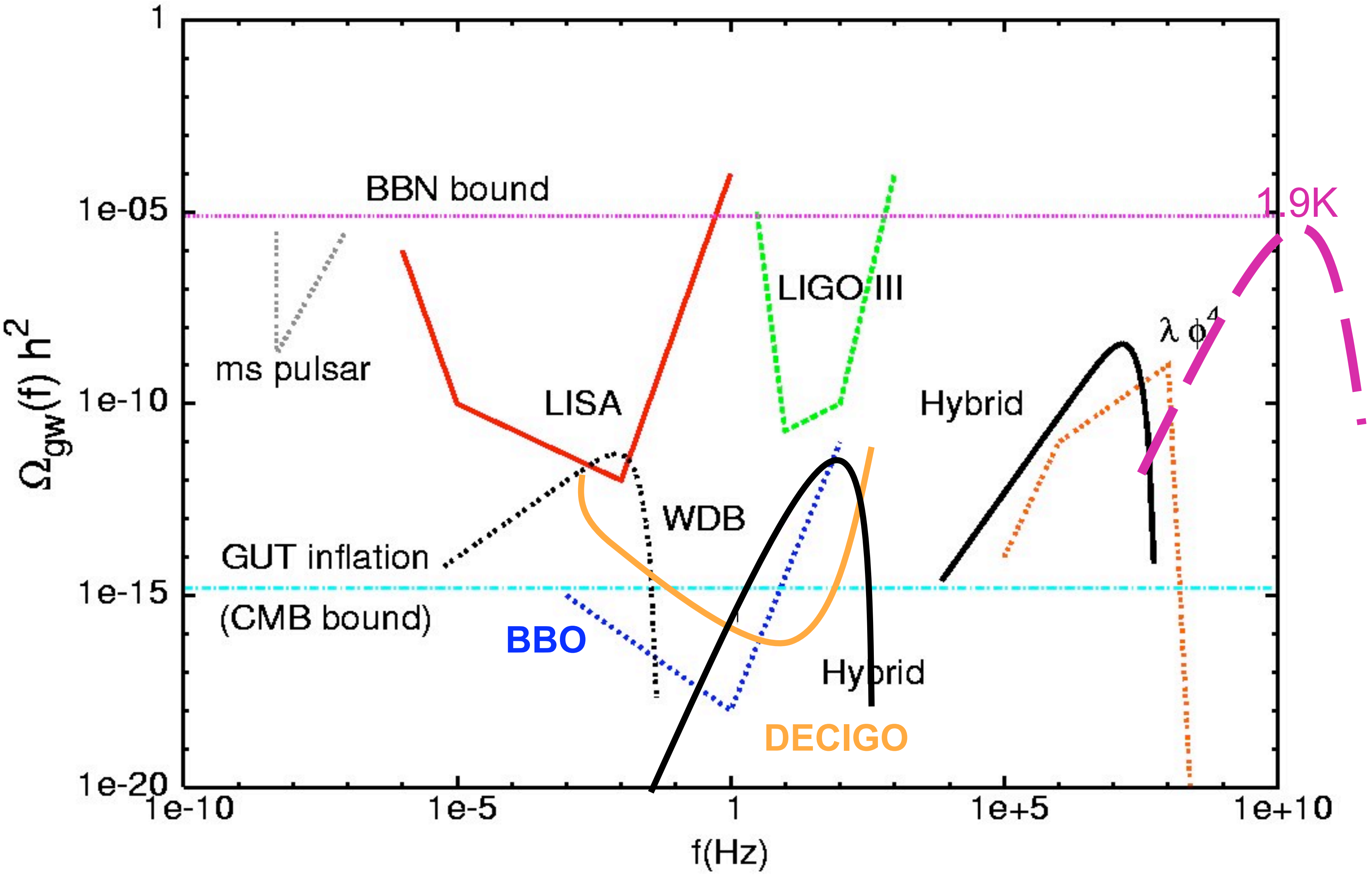

Gravitational waves from Abelian-Higgs model

J. G.-B.
Daniel Garcia Figueroa
Jeff Dufaux

arXiv:1005.1234

The Abelian Higgs-Inflaton model

$$L = -\frac{1}{4} F^a_{\mu\nu} F_a^{\mu\nu} + Tr[(D_\mu \Phi)^+ D^\mu \Phi] + \frac{1}{2}(\partial_\mu \chi)^2 - V(\Phi, \chi)$$

$$D_\mu = \partial_\mu - ieA_\mu \qquad F_{\mu\nu} = \partial_\mu A_\nu - \partial_\nu A_\mu$$

$$Tr[\Phi^+ \Phi] = \frac{1}{2}(\phi^a \phi_a) \equiv \frac{1}{2}\phi^2$$

$$V(\phi, \chi) = \frac{\lambda}{4}(\phi^2 - v^2)^2 + \frac{g^2}{2}\phi^2 \chi^2 + \frac{1}{2} m^2 \chi^2$$

$$g_{\mu\nu} = \eta_{\mu\nu} + h_{\mu\nu}, \quad h_{\mu 0} = 0, \quad \nabla^i h_{ij} = 0, \quad h^i_i = 0$$

$$g^{\mu\nu} \partial_\mu \phi \, \partial_\nu \phi = (\partial_0 \phi)^2 - (\nabla \phi)^2 \underline{- h^{ij} \nabla_i \phi \, \nabla_j \phi}$$

including backreaction

Evolution of Higgs histograms

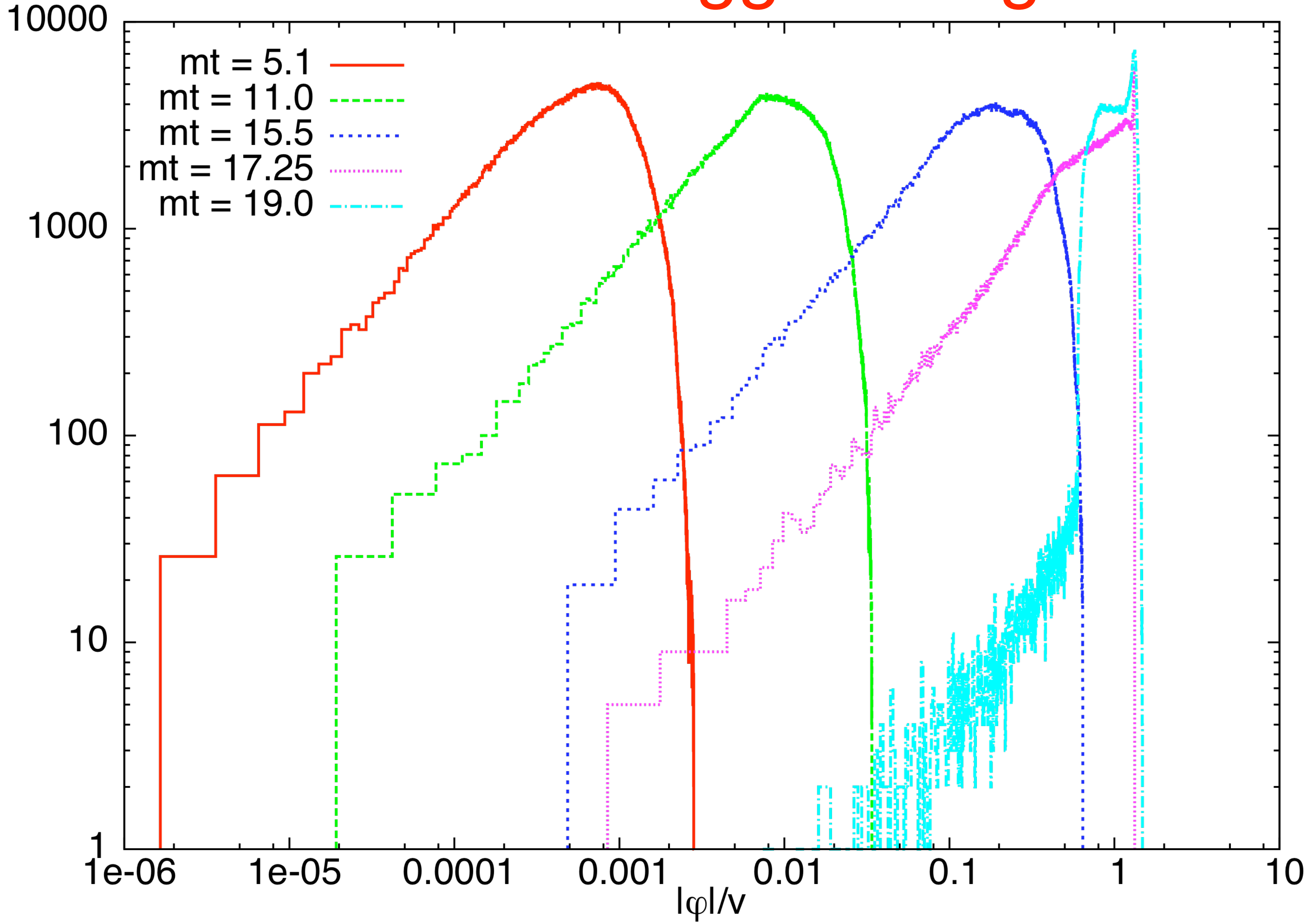

Evolution of Higgs histograms

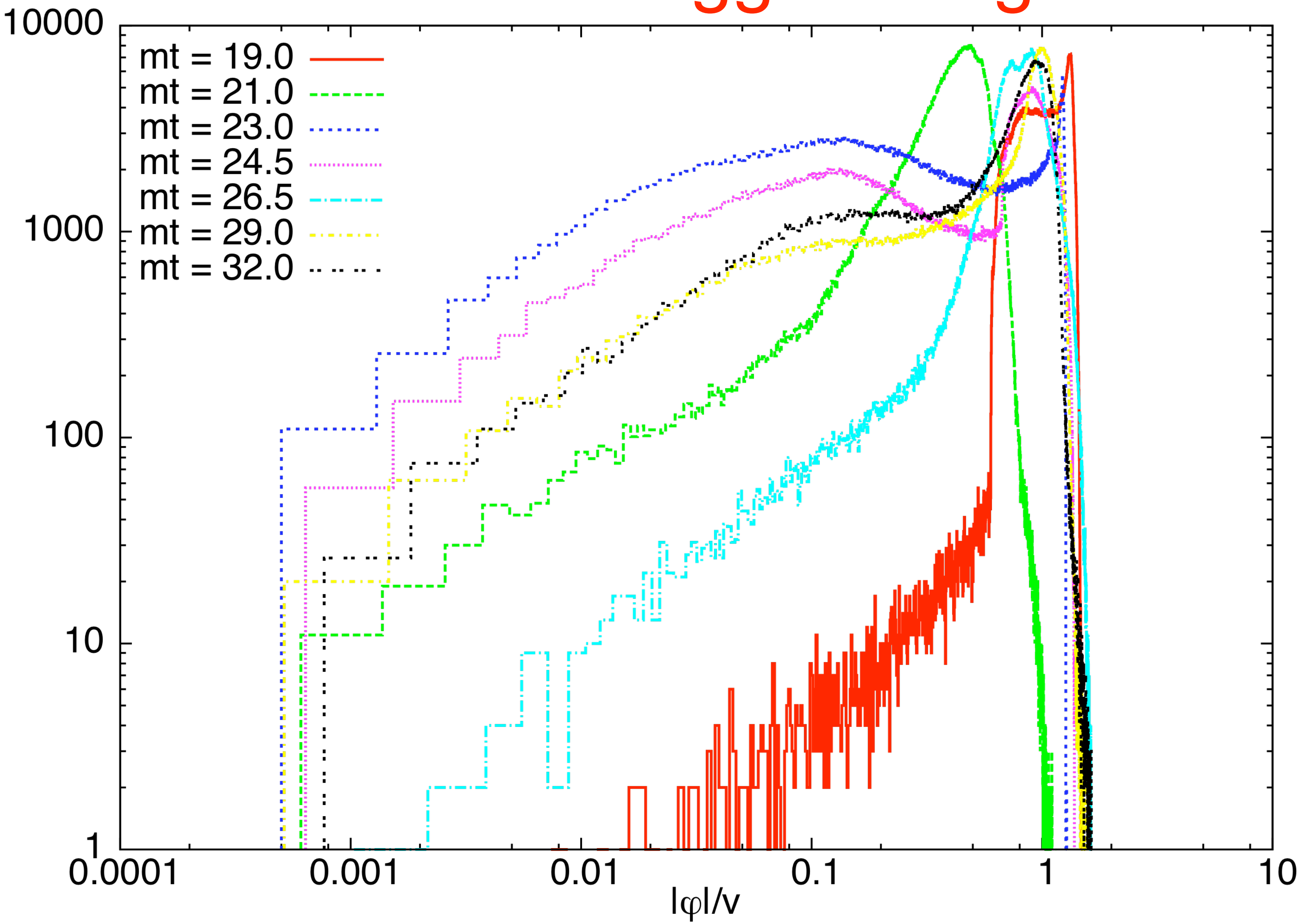

Evolution of Higgs histograms

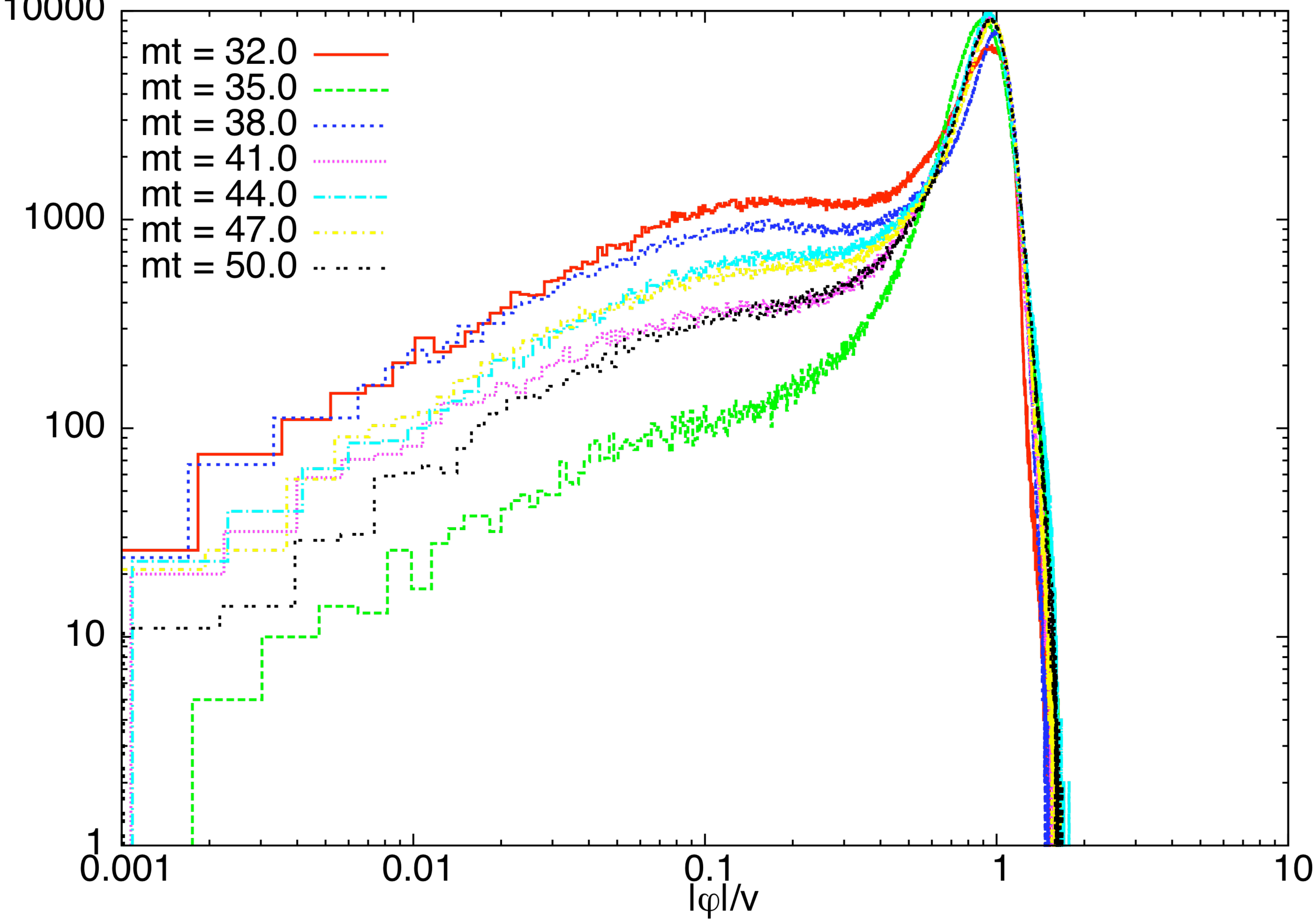

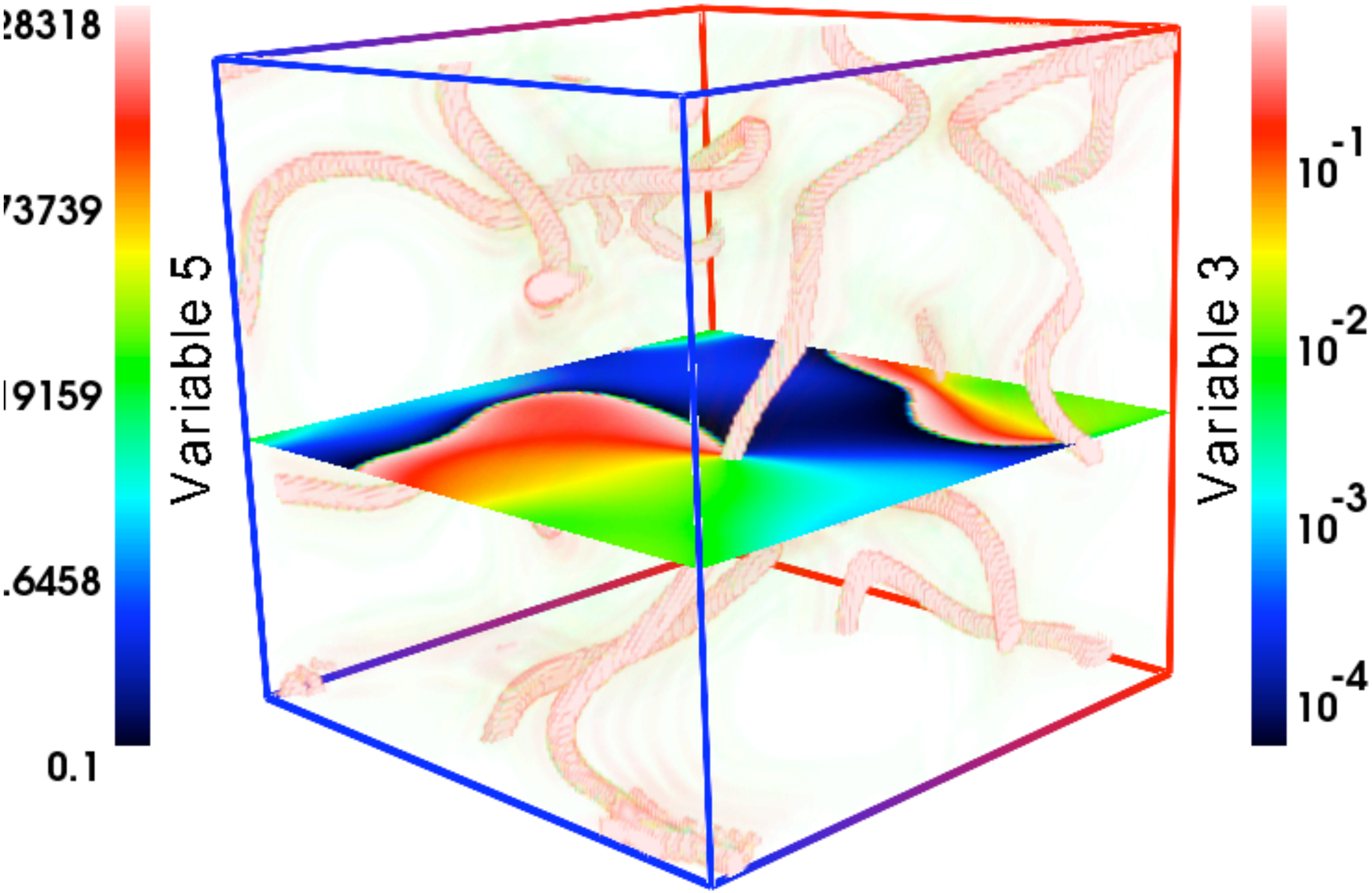

28318
73739
19159
.6458
0.1
Variable 5
Variable 3
10^{-1}
10^{-2}
10^{-3}
10^{-4}

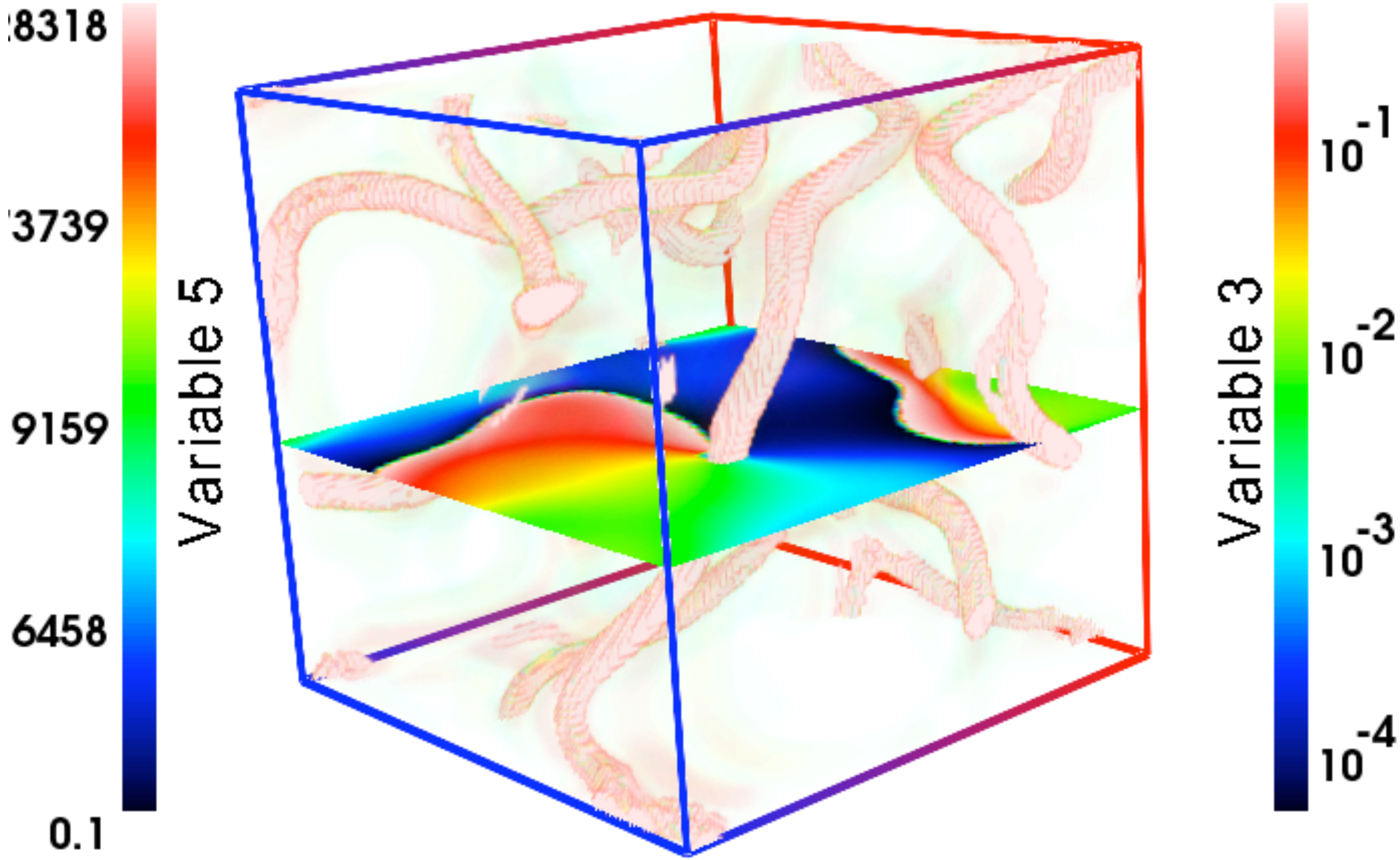

28318
3739
9159
6458
0.1
Variable 5
Variable 3
10^{-1}
10^{-2}
10^{-3}
10^{-4}

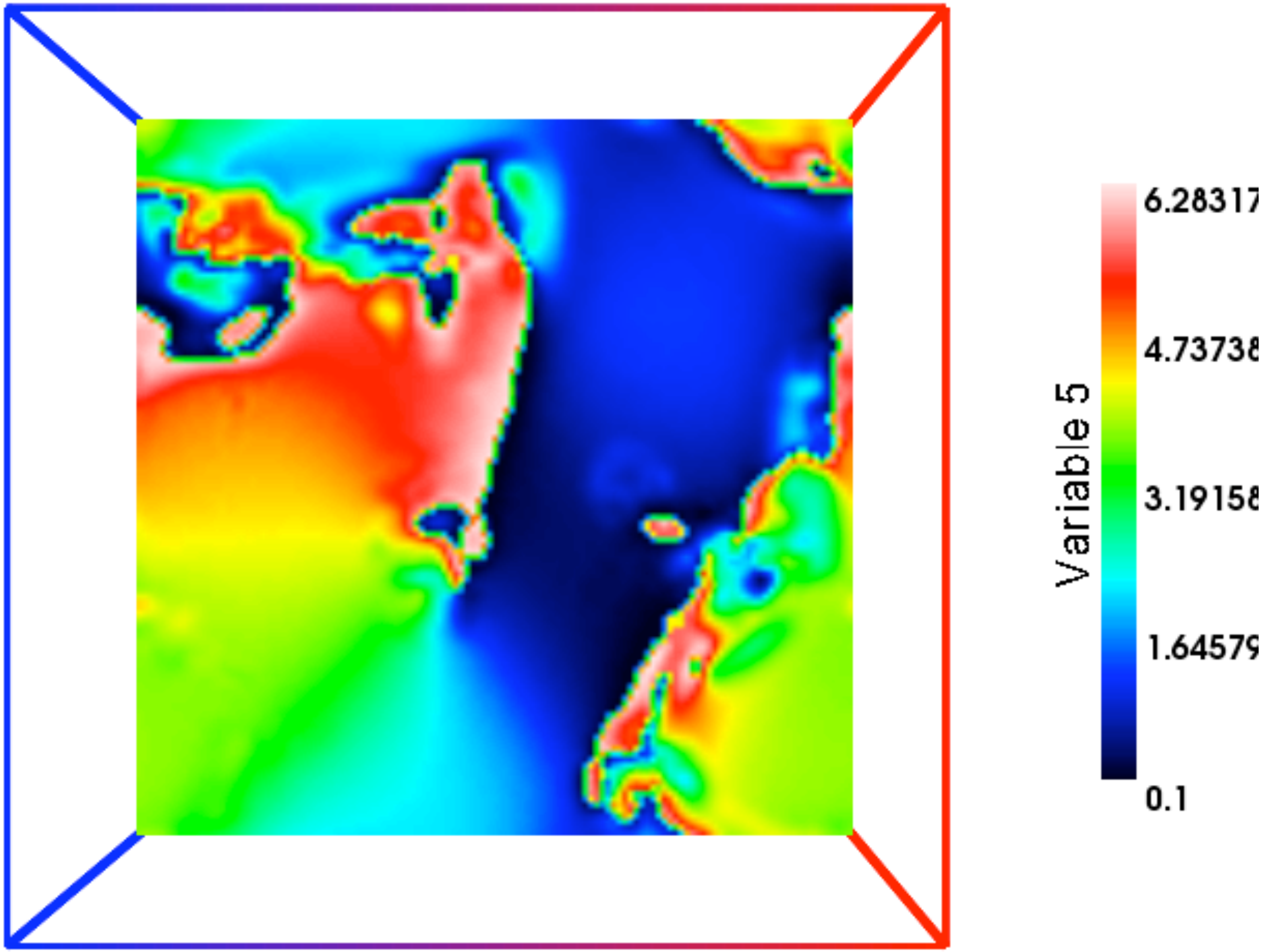
6.28317
4.73738
3.19158
1.64579
0.1
Variable 5

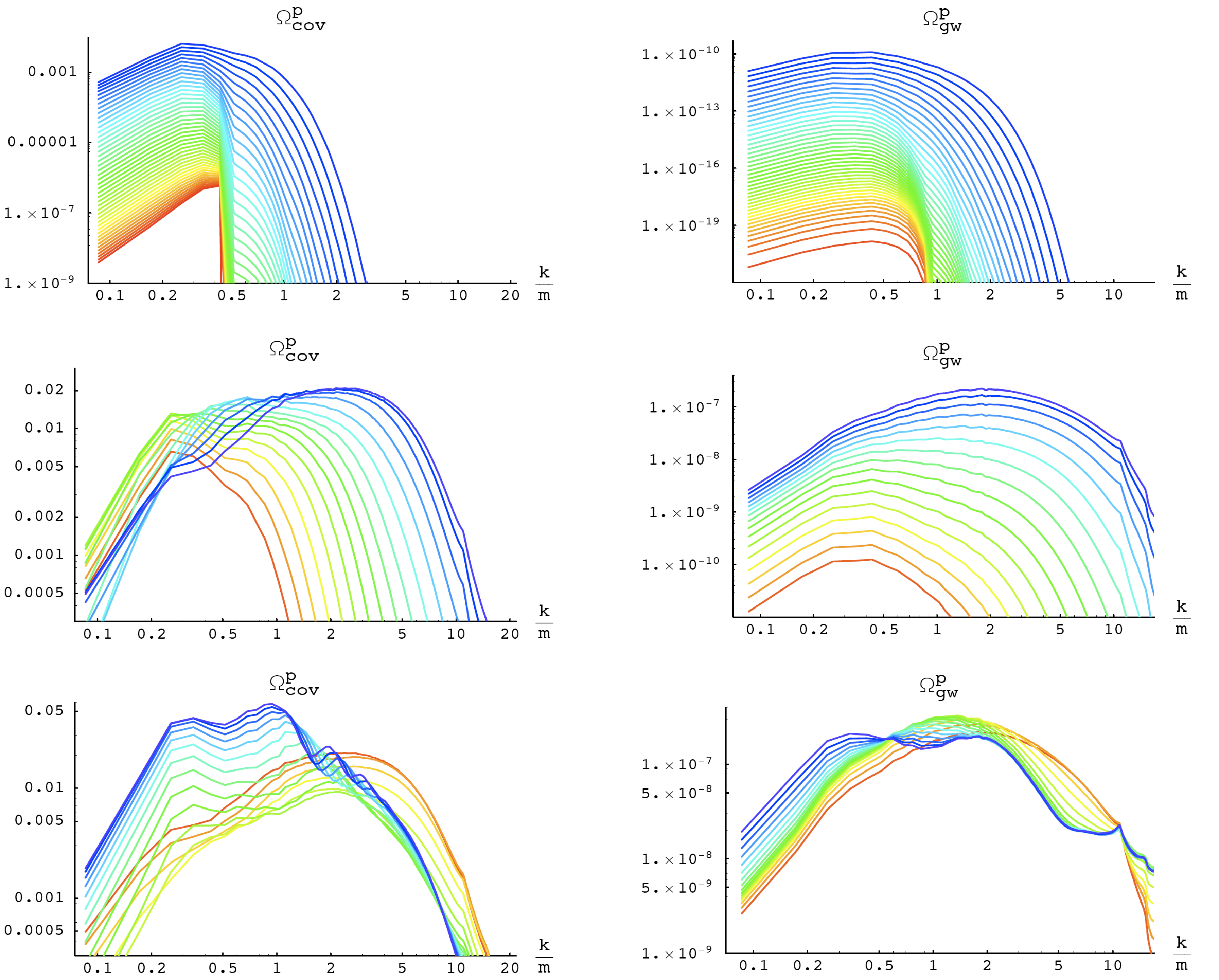
Ωpcov
0.001
0.00001
1. × 10−7
1. × 10−9
0.1 0.2 0.5 1 2 5 10 20
k/m
Ωpgw
1. × 10−10
1. × 10−13
1. × 10−16
1. × 10−19
0.1 0.2 0.5 1 2 5 10
k/m
Ωpcov
0.02
0.01
0.005
0.002
0.001
0.0005
0.1 0.2 0.5 1 2 5 10 20
k/m
Ωpgw
1. × 10−7
1. × 10−8
1. × 10−9
1. × 10−10
0.1 0.2 0.5 1 2 5 10
k/m
Ωpcov
0.05
0.01
0.005
0.001
0.0005
0.1 0.2 0.5 1 2 5 10 20
k/m
Ωpgw
1. × 10−7
5. × 10−8
1. × 10−8
5. × 10−9
1. × 10−9
0.1 0.2 0.5 1 2 5 10
k/m

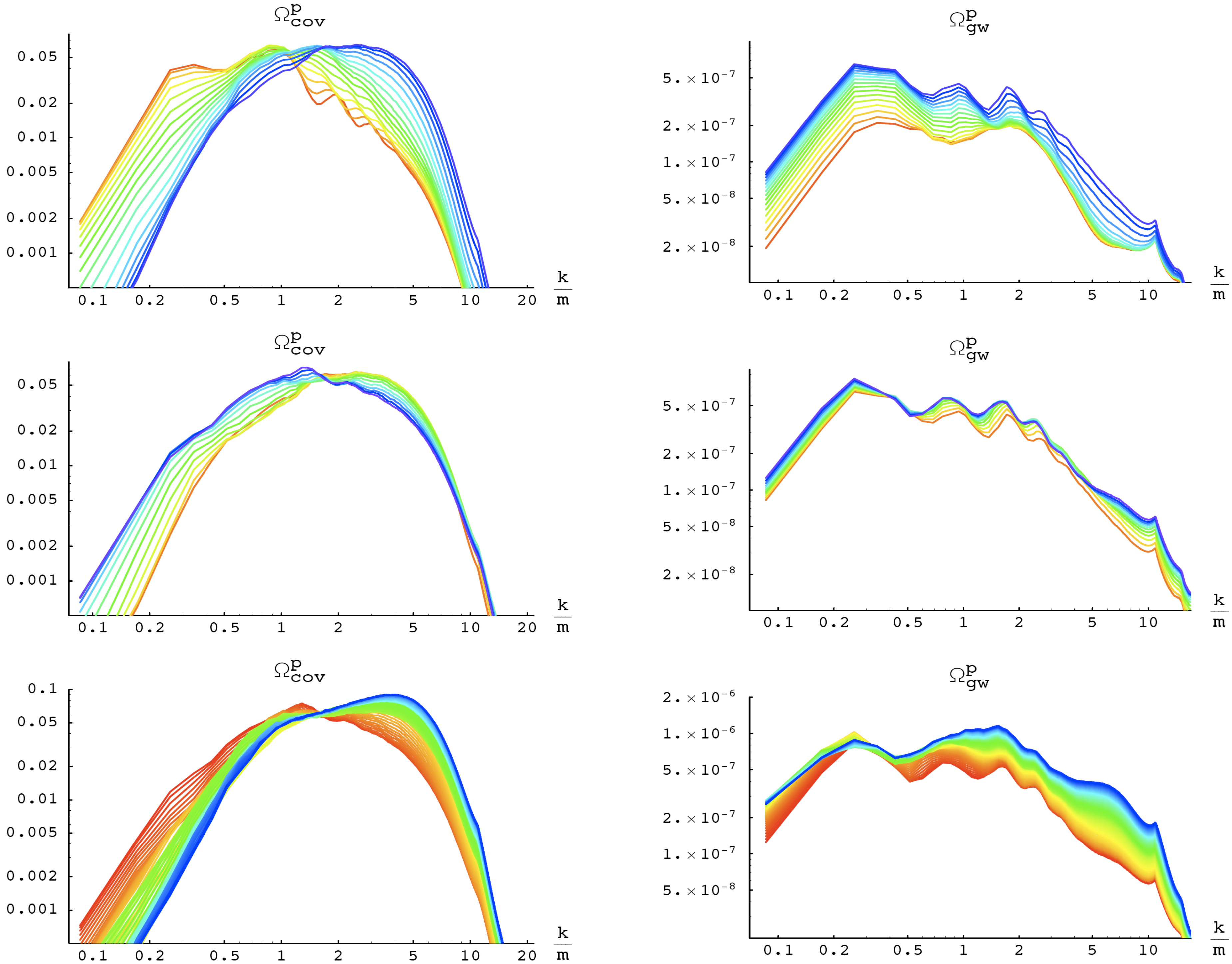

Ω^p_cov
Ω^p_gw
0.05
0.02
0.01
0.005
0.002
0.001
0.1
0.2
0.5
1
2
5
10
20
k
m
5.×10^-7
2.×10^-7
1.×10^-7
5.×10^-8
2.×10^-8
2.×10^-6
1.×10^-6

Evolution of GW background

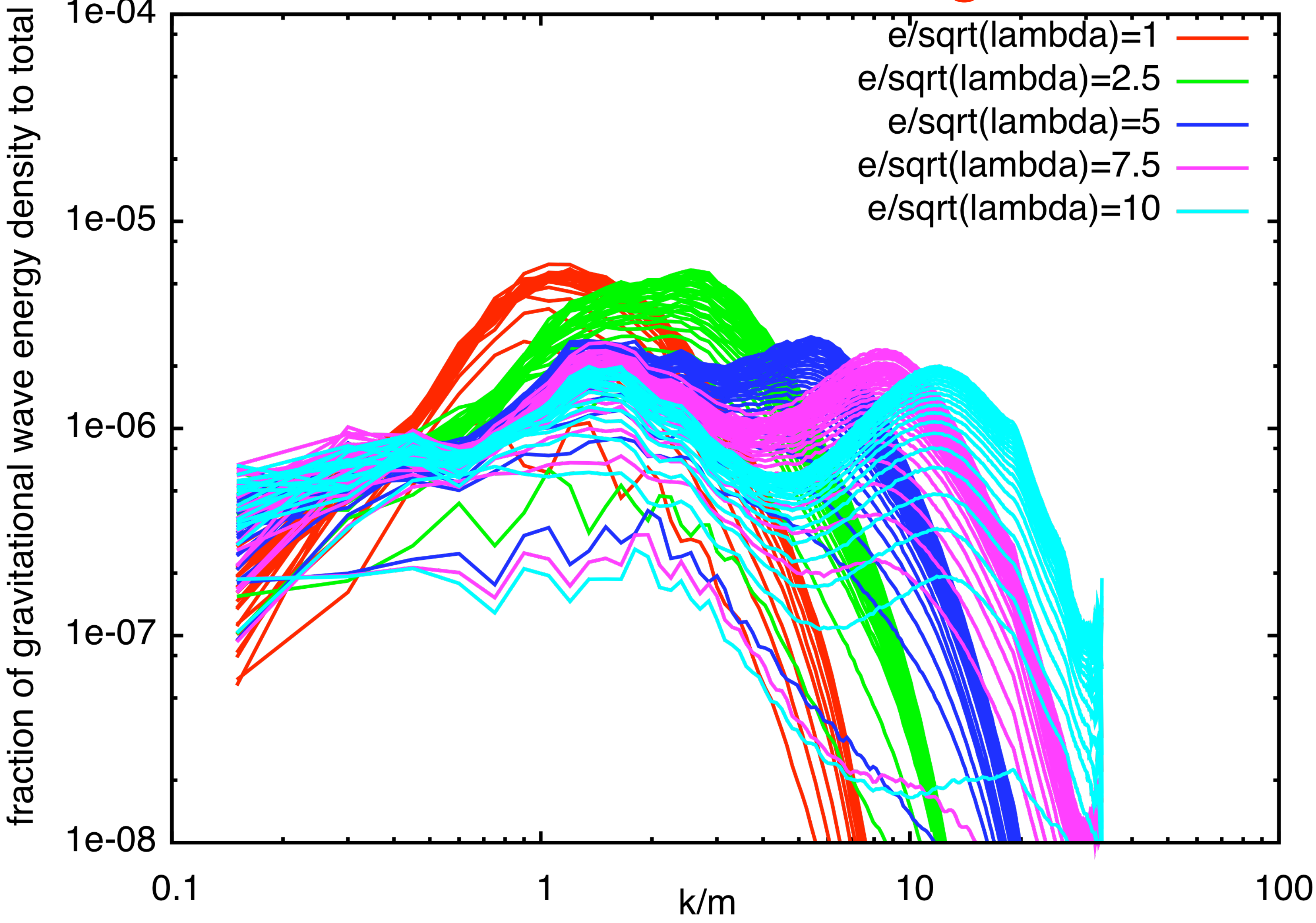

Higgs covariant gradient energy

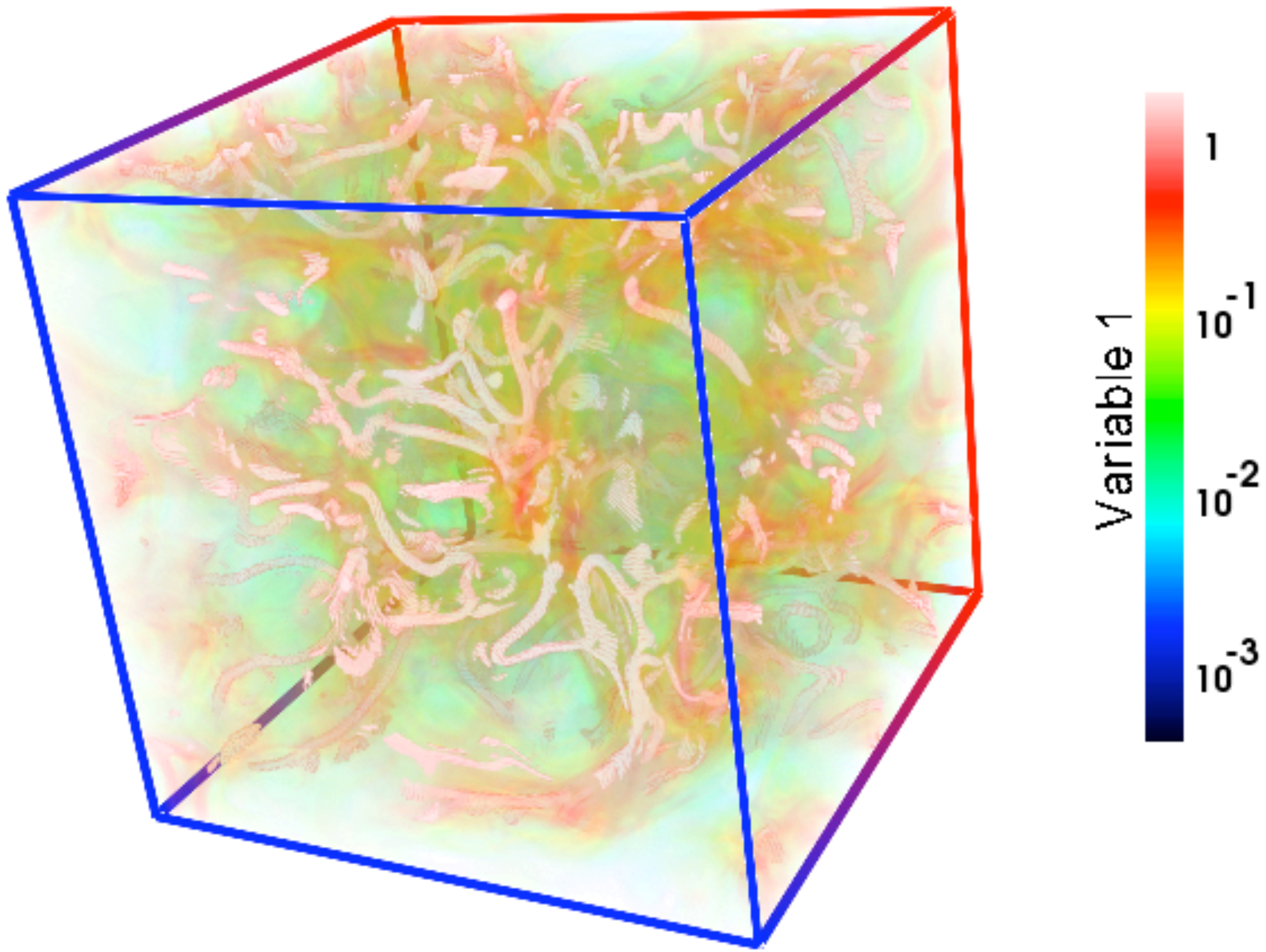

Magnetic energy density

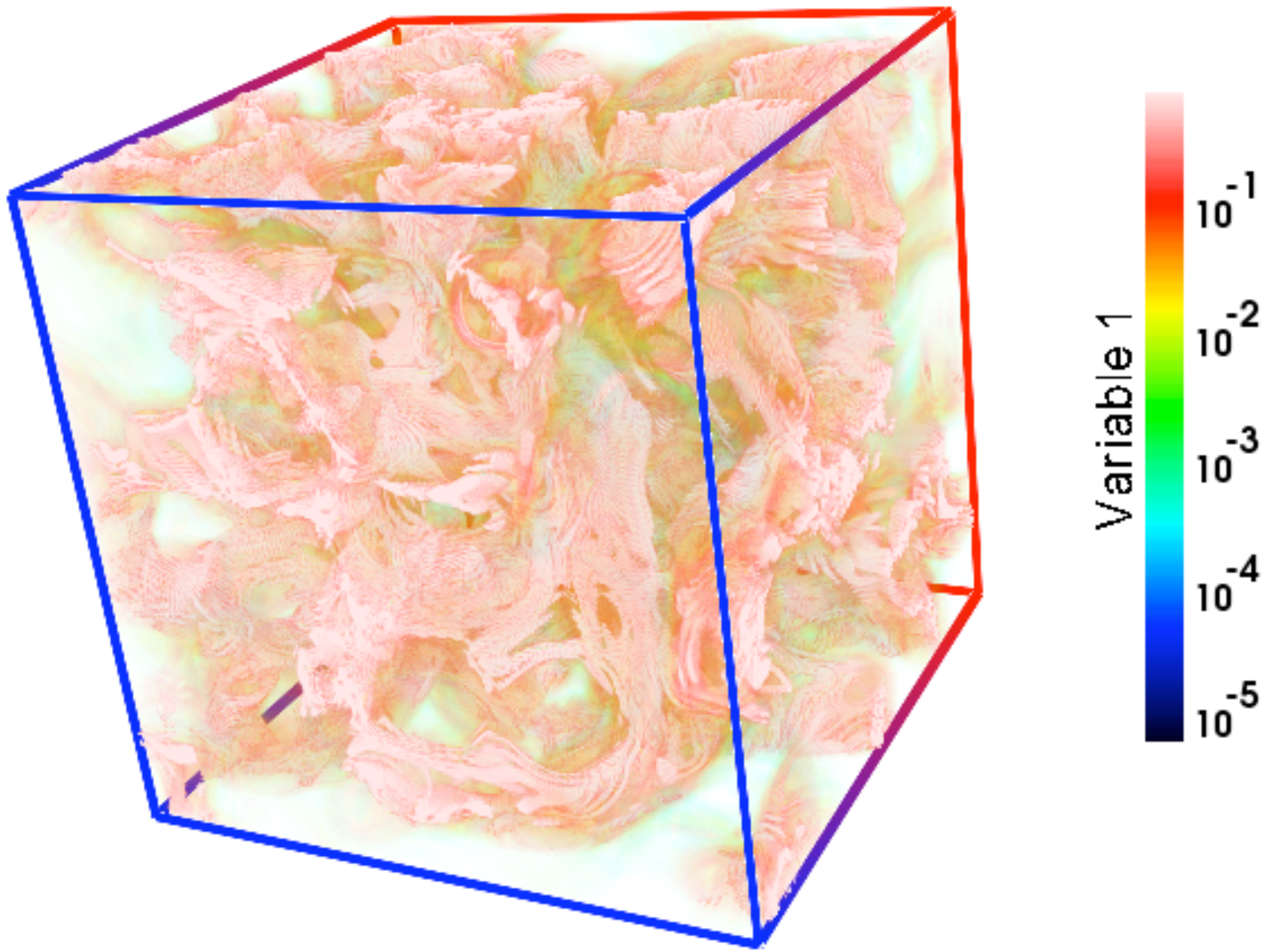

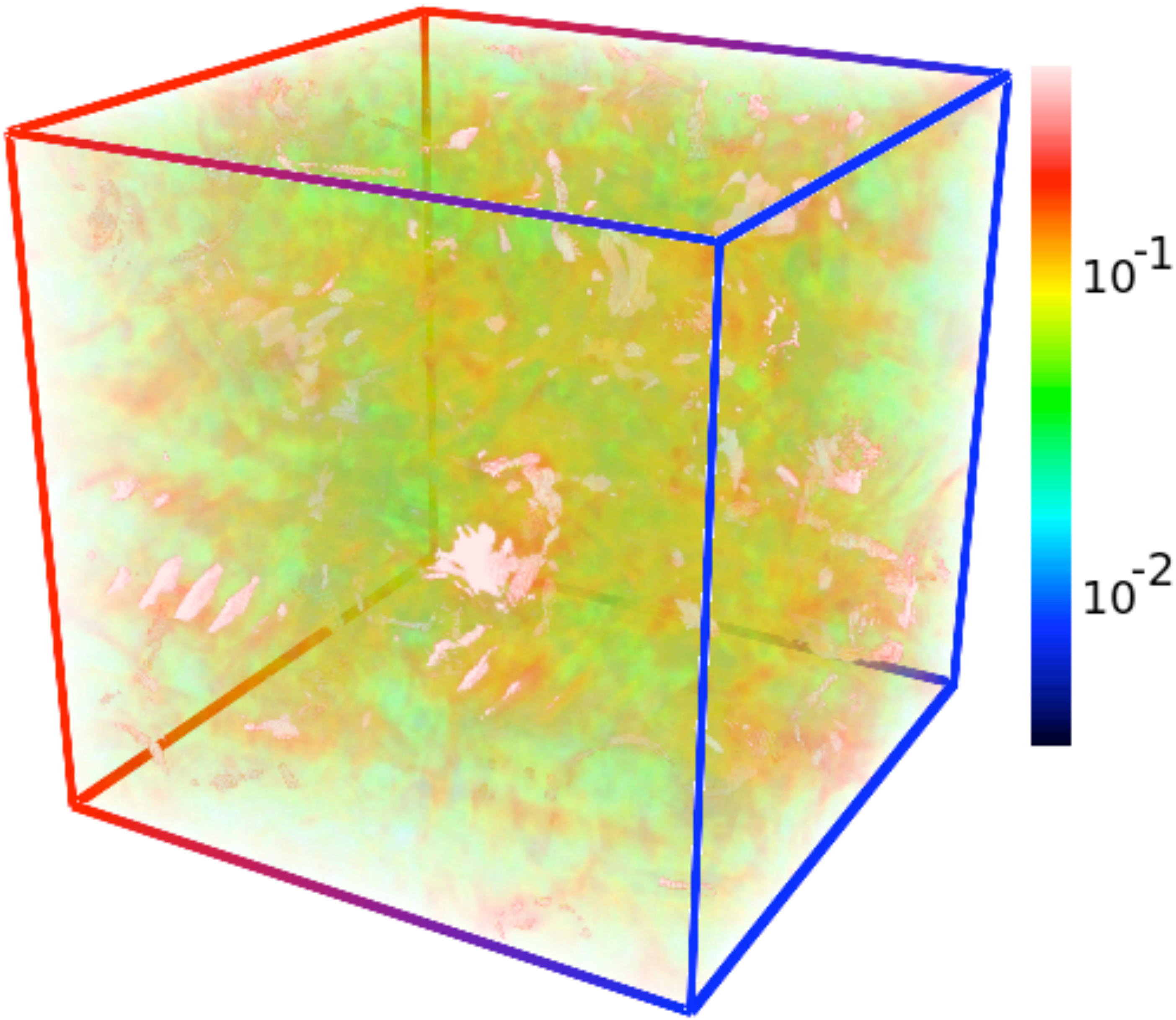

Gravitational waves energy density

Gravitational waves energy density

Dufaux, Figueroa, JGB arXiv:1006.02171

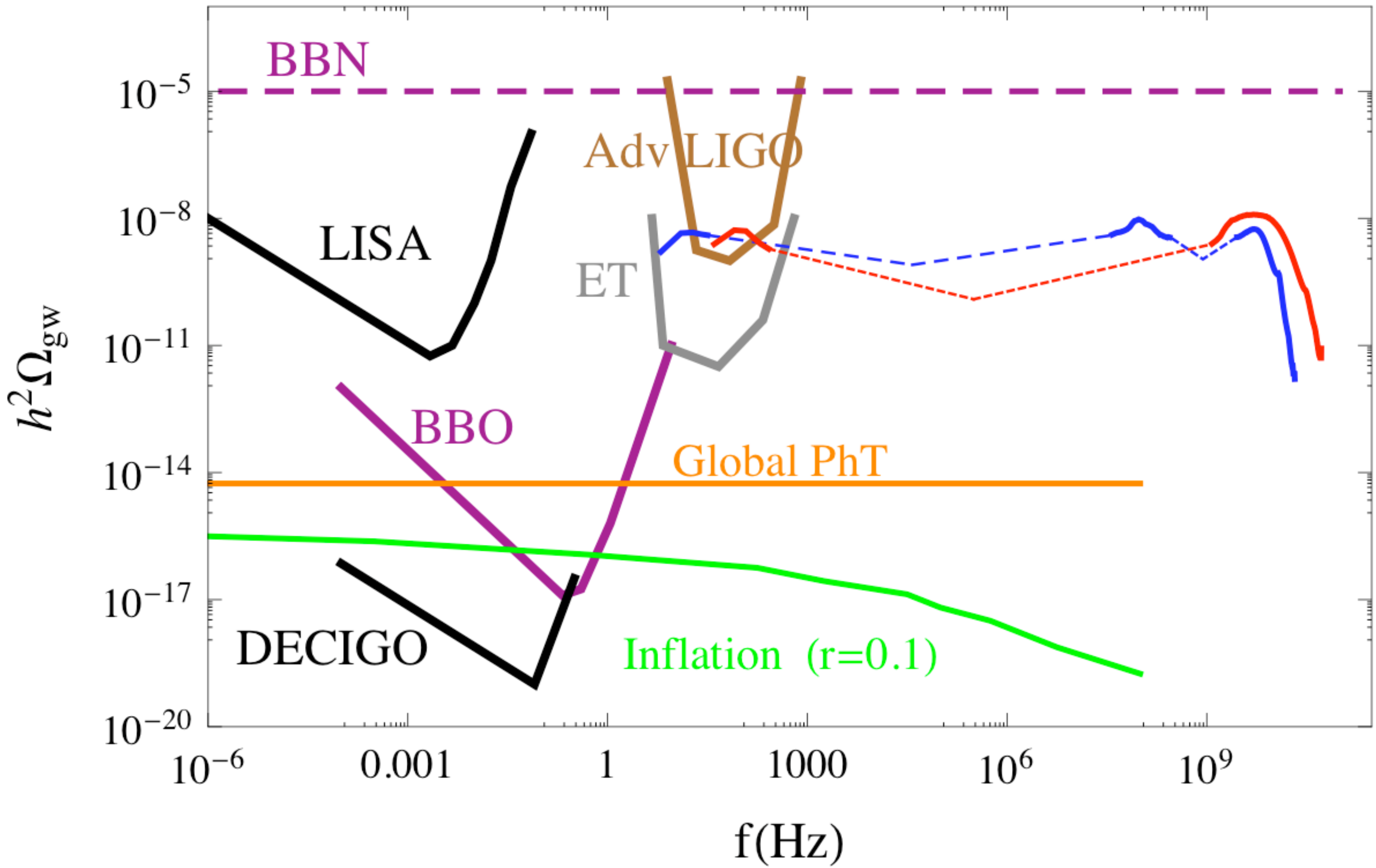

Gravitational waves sky maps

Thrane et al. PRD80, 122002 (2009)

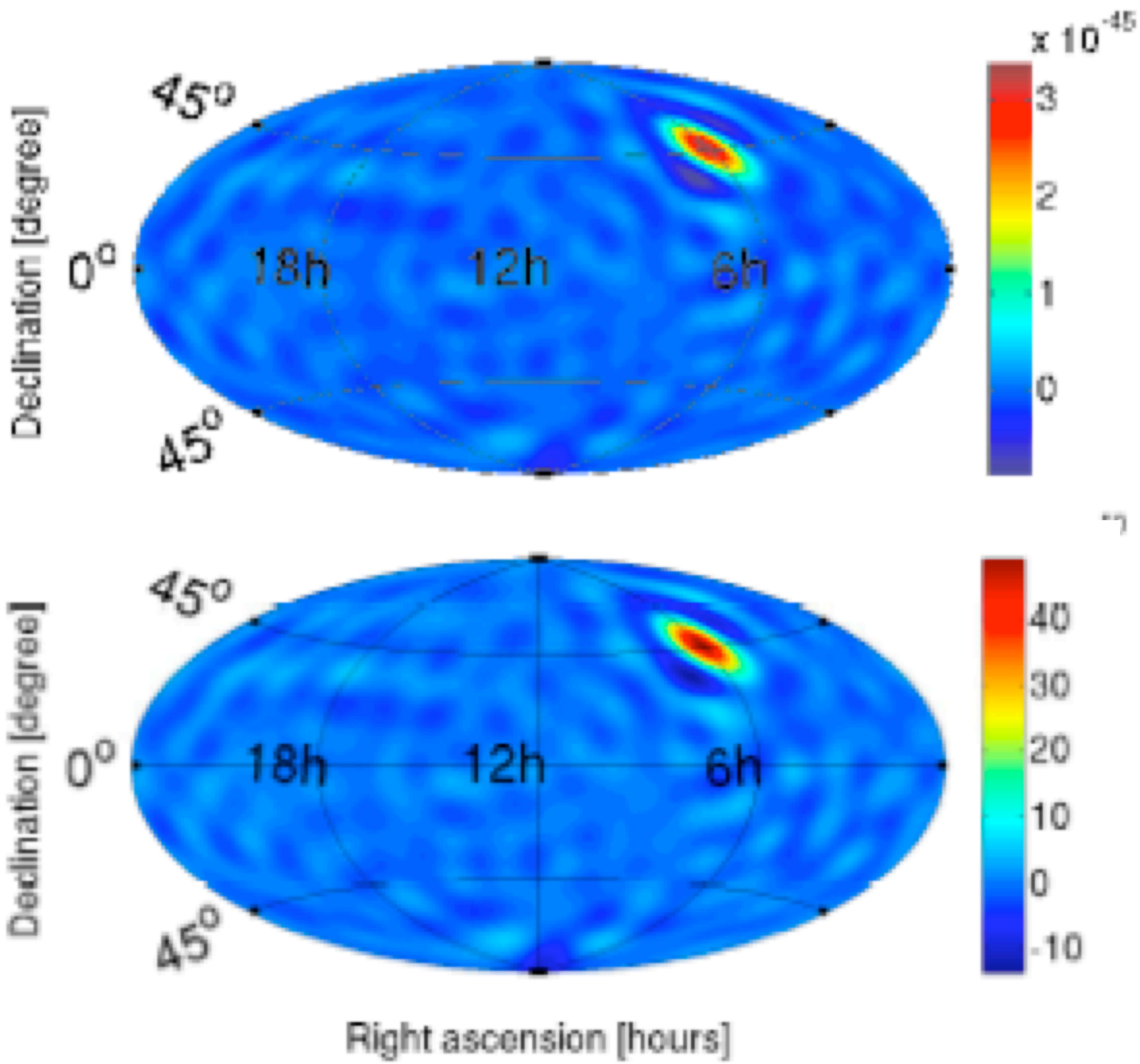

Point source @ (6hr, +45deg)

clean

SNR=49
lmax=20

Gravitational waves sky maps

Thrane et al. PRD80, 122002 (2009)

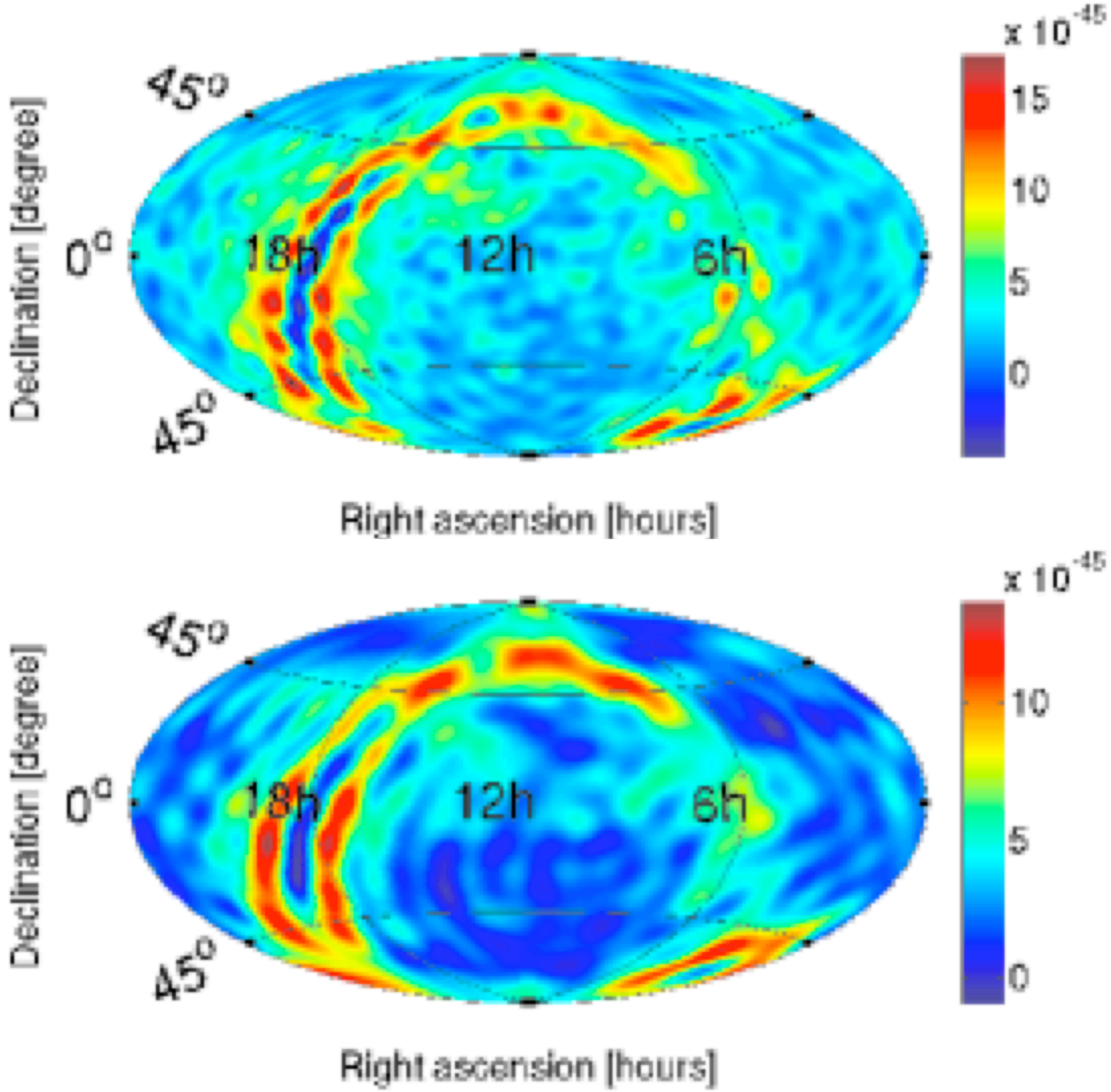

clean

Ecuatorial injection

dirty

Another source of GW

Gravitational waves from self-ordering fields

Elisa Fenu
Daniel G. Figueroa
Ruth Durrer
JGB

JCAP 0910, 005 (2009)
arXiv:1003.0299

L.Krauss
PLB284,229 (1992)

Jones-Smith et al.
PRL100, 131302 (2008)

Non-linear sigma model

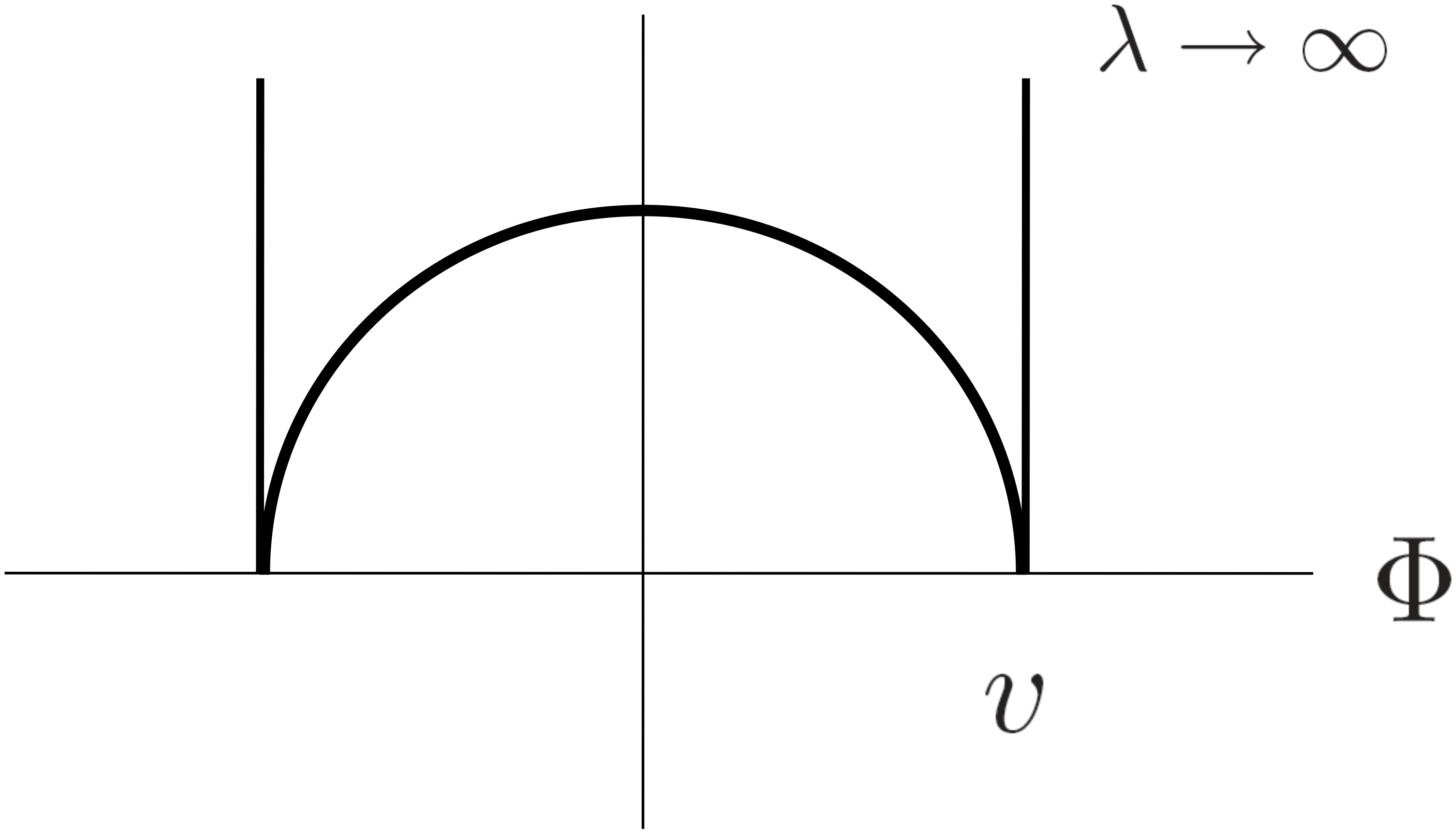

self-ordering of Goldstone modes on large scales

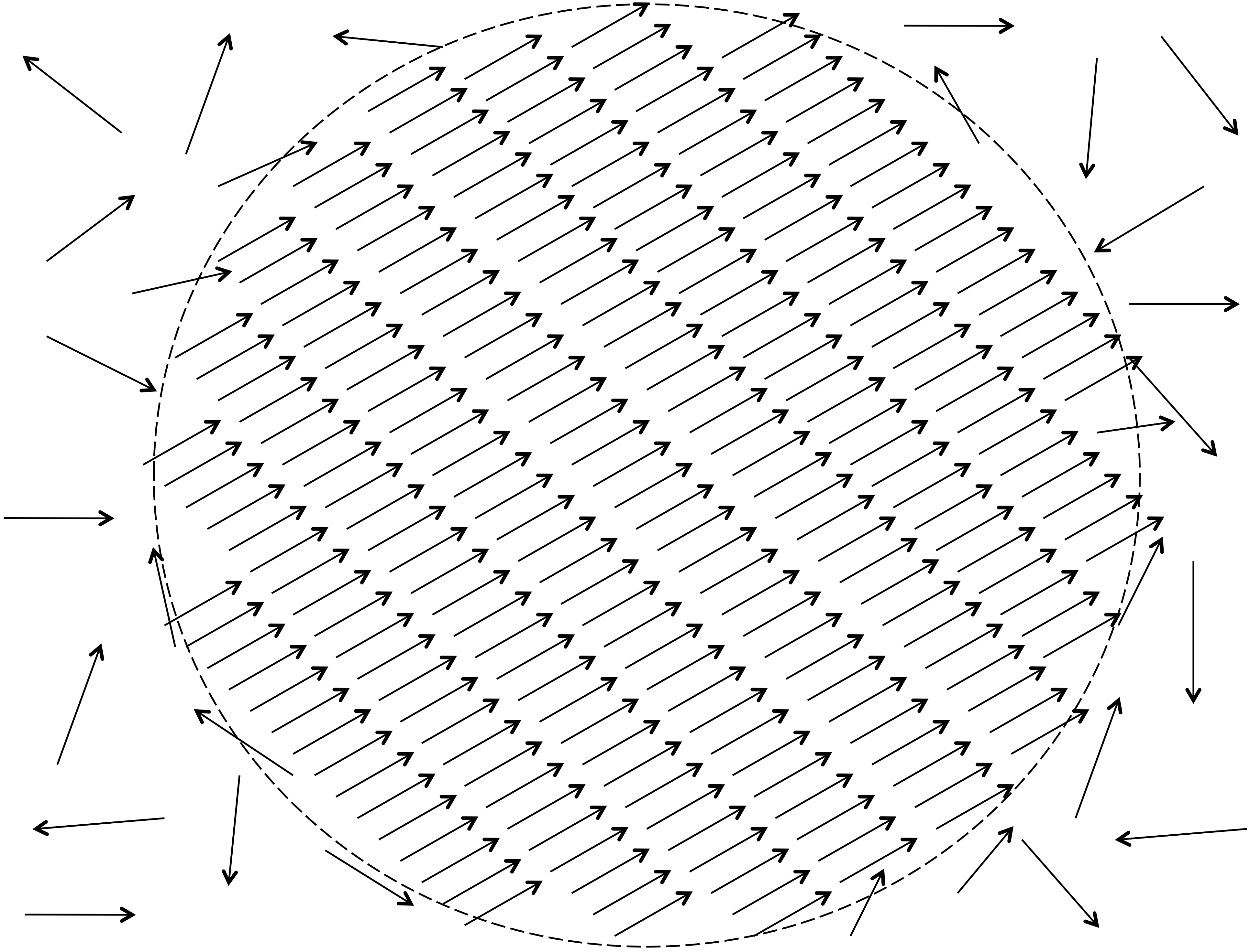

GW multiple origins for hybrid models

preheating

- small scales (subhorizon)
- anisotropic stresses from bubble collisions and kinetic turbulence
- GW power peaked at k~m
- relevant d.o.f. is Higgs
- spinodal growth of modes
- exact tachyonic solutions
- lasts for short time of SB
- don't induce density pert. on large scales
- can be observed @ BBO

self-ordering

- large scales (superhorizon)
- anisotropic stresses from field realignment and spatial gradients
- GW power peaked at k~H
- d.o.f. Goldstone modes
- self-ordering fields
- exact scaling solutions
- never stops
- produces also scalar and vector perturbations
- can be observed @ CMB

Gravitational wave power spectrum

$$\frac{d\rho_{\rm GW}(k,\eta)}{d\log k} = \frac{G\,v^4}{4\pi^4}\frac{k^3}{a^4(\eta)}\frac{36\pi^4 A^2}{N}\int_{\eta_*}^{\eta} d\tau \int_{\eta_*}^{\eta} d\xi\ a(\tau)a(\xi)\ \cos(k\xi - k\tau)$$

$$\times \int_{\substack{p\,<\,1/\eta_* \\ |\mathbf{k}-\mathbf{p}|\,<\,1/\eta_*}} d^3p\ p^4 \sin^4\theta\ \tau^3\xi^3\ \frac{J_\nu(p\tau)}{(p\tau)^\nu}\frac{J_\nu(p\xi)}{(p\xi)^\nu}\frac{J_\nu(|\mathbf{k}-\mathbf{p}|\tau)}{(|\mathbf{k}-\mathbf{p}|\tau)^\nu}\frac{J_\nu(|\mathbf{k}-\mathbf{p}|\xi)}{(|\mathbf{k}-\mathbf{p}|\xi)^\nu}$$

$$\Omega_{\rm GW}(k,\eta) = \frac{G^2 v^4 \Omega_{\rm rad}}{N a^4(\eta)}\,75\pi^4\int_0^\infty dq\, q^2 F(q)\left\{\left[\int_0^{k\eta} dx\ \cos x\ J_2^2(qx)\right]^2 + \left[\int_0^{k\eta} dx\ \sin x\ J_2^2(qx)\right]^2\right\}$$

$$F(q) = \int_{-1}^{1}\frac{du\,(1-u^2)^2}{(q^2+1-2qu)^2} = \frac{1}{24q^5}\left[16q + 12q(q^2-1)^2 + 3(q^2-1)^2(q^2+1)\log\frac{(q-1)^2}{(q+1)^2}\right]$$

$$a(\eta) \simeq H_0\sqrt{\Omega_{\rm rad}}\,\eta \qquad \text{consistent with } a_0 = 1 \text{ today}$$

$$\Omega_{\rm GW}(k,\eta_0) \simeq \frac{511}{N}\Omega_{\rm rad}\left(\frac{v}{M_{\rm Pl}}\right)^4$$

scale invariant spectrum

GW density parameter today

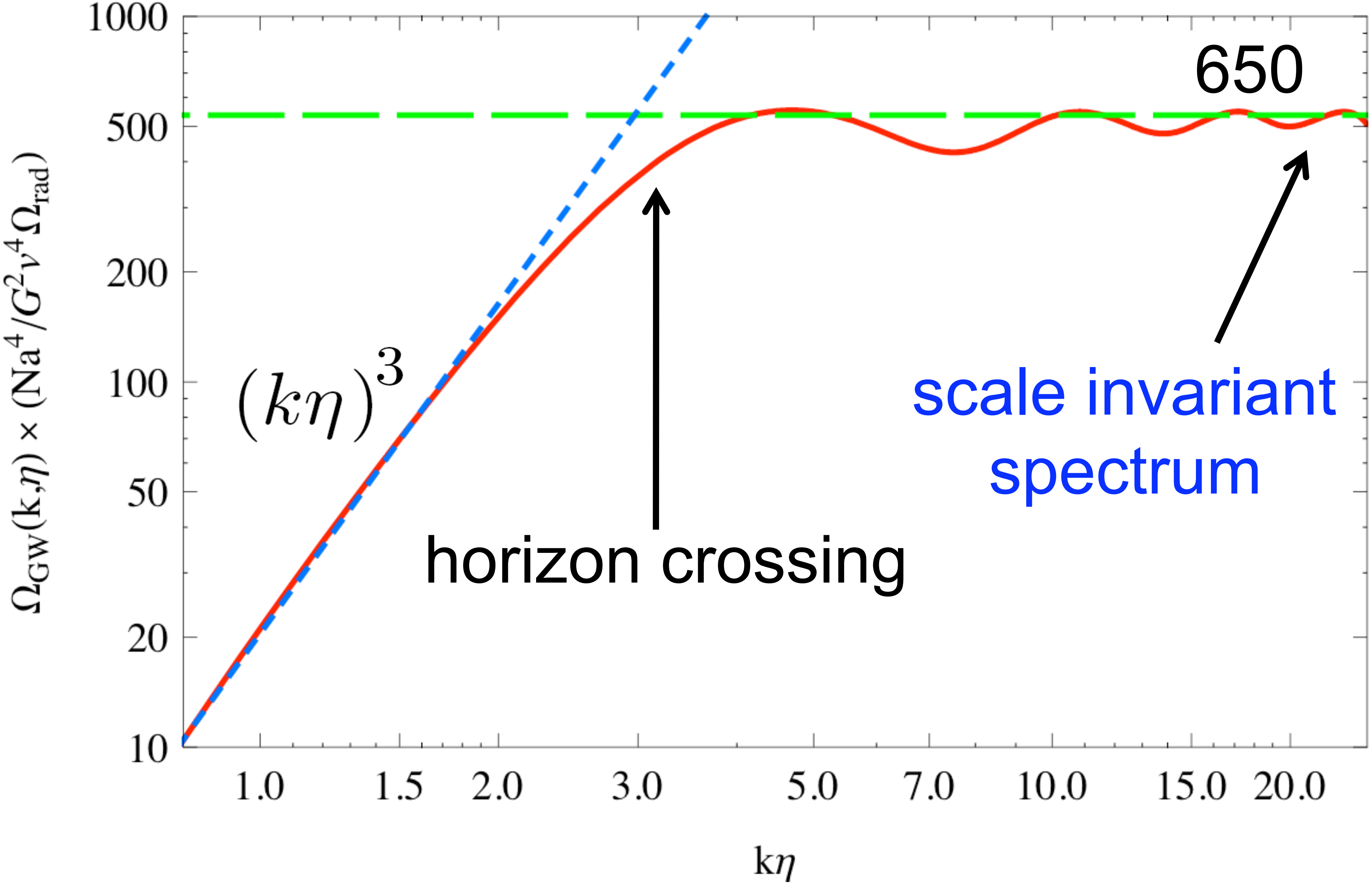

Observational bounds on GW

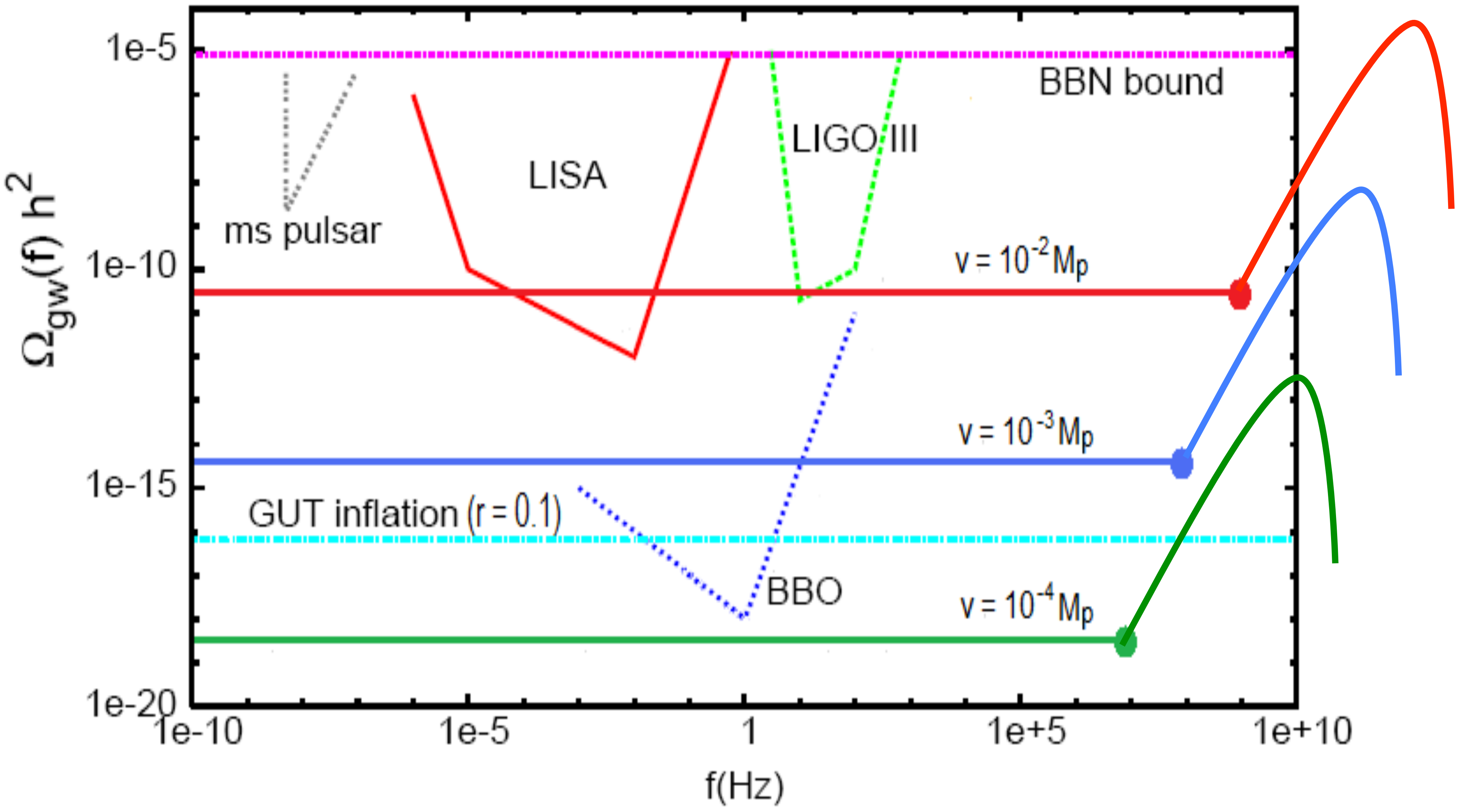

Distinguishing GWs in CMB polarization anisotropies

Polarization basics

$$(\mathbf{e}^{(1)}, \mathbf{e}^{(2)}, \mathbf{n}) \qquad \text{right-handed orthonormal}$$

$$\mathbf{E} = E_1\,\mathbf{e}^{(1)} + E_2\,\mathbf{e}^{(2)} \qquad \text{electric field}$$

$$P_{ij} = \mathcal{P}_{ab}\,e_i^{(a)}\,e_j^{(b)} \qquad \text{polarization tensor}$$

$$\mathcal{P}_{ab} = E_a^* E_b = \frac{1}{2}\left[I\sigma_{ab}^{(0)} + U\sigma_{ab}^{(1)} + V\sigma_{ab}^{(2)} + Q\sigma_{ab}^{(3)}\right]$$

Stokes parameters

$$I = |E_1|^2 + |E_2|^2 \qquad Q = |E_1|^2 - |E_2|^2$$

$$U = 2\mathrm{Re}(E_1^* E_2) \qquad V = 2\mathrm{Im}(E_1^* E_2) = 0$$

Thomson scattering does not induce circular polarization

$$\mathbf{e}_\pm = \frac{1}{\sqrt{2}}(\mathbf{e}_1 \pm i\mathbf{e}_2) \qquad \text{circular polarization vectors}$$

$$P_{\pm\pm} = 2\mathbf{e}^a_\pm \mathbf{e}^b_\pm P_{ab} = Q \pm iU$$

$$P_{+-} = P_{-+} \propto V = 0$$

$$\mathcal{P}_{ab} = \frac{1}{2} I\delta_{ab} + P_{ab}$$

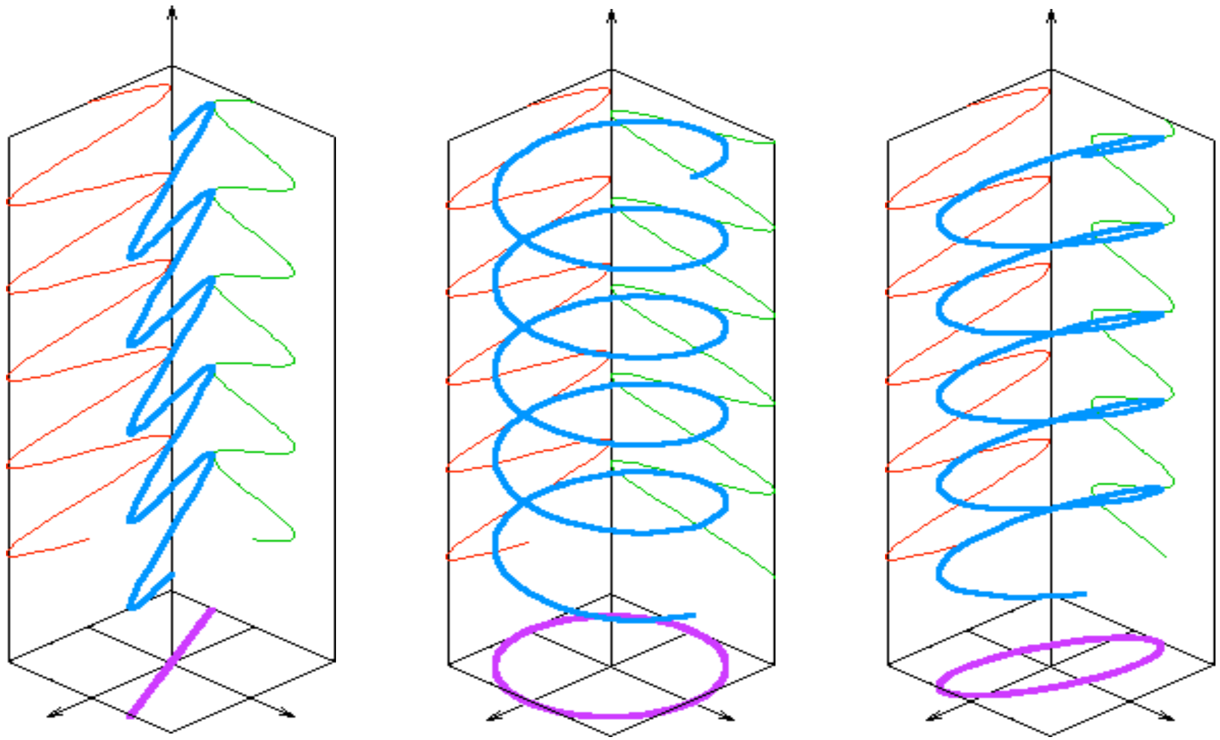

linear circular elliptical

polarization types

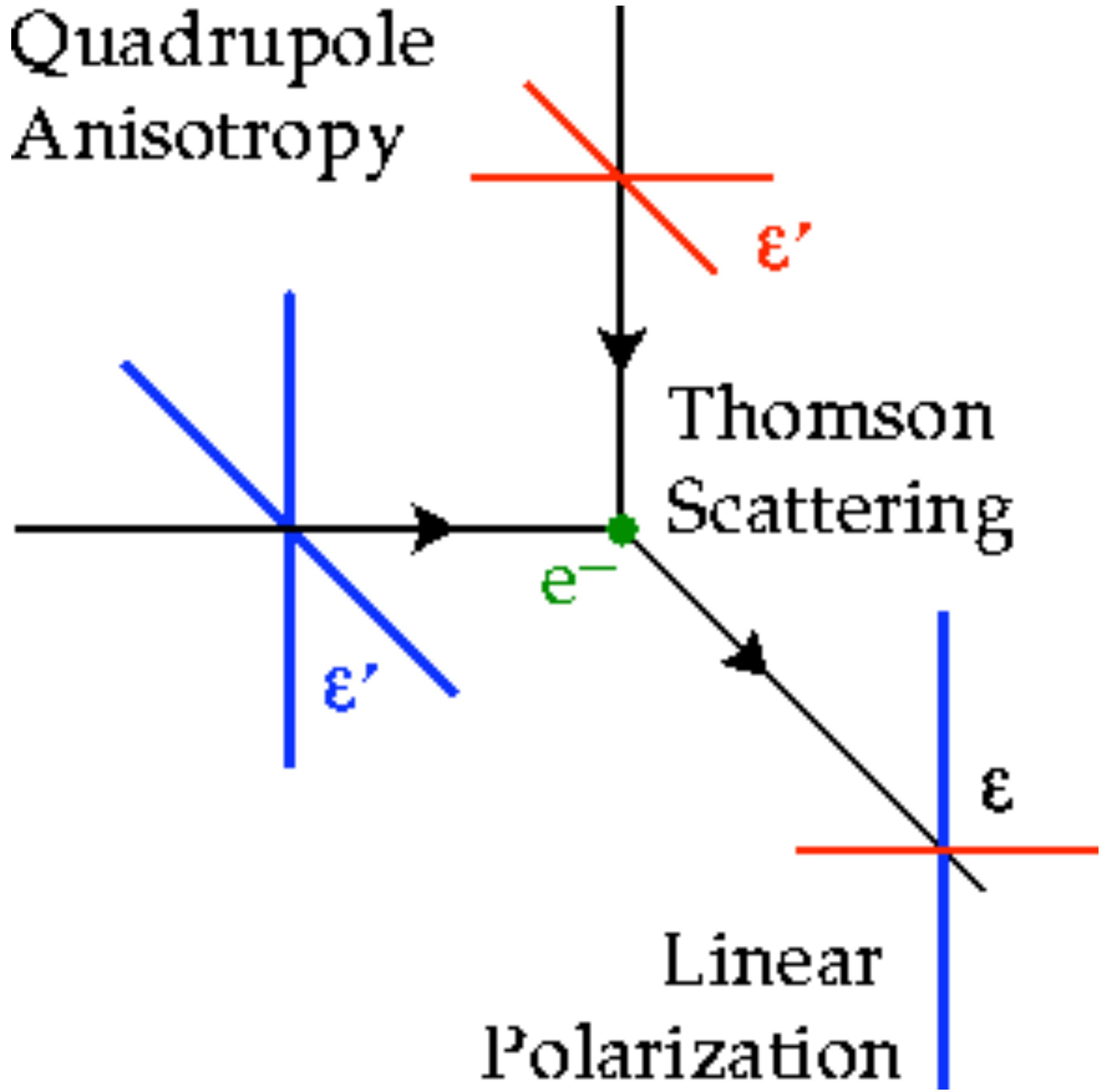
Quadrupole
Anisotropy
ε′
Thomson
Scattering
e⁻
ε′
ε
Linear
Polarization

Polarization around Hot spots

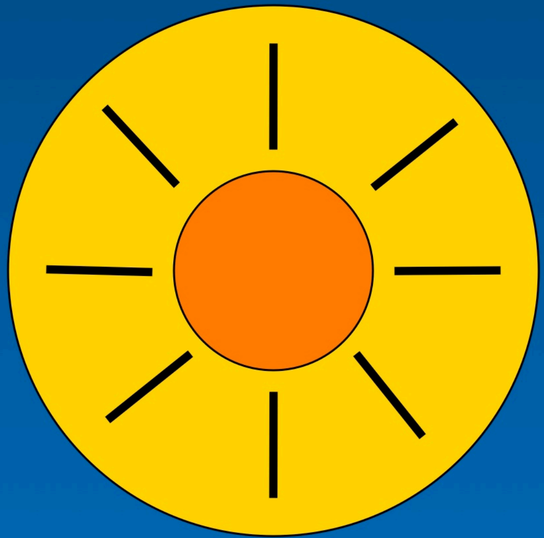

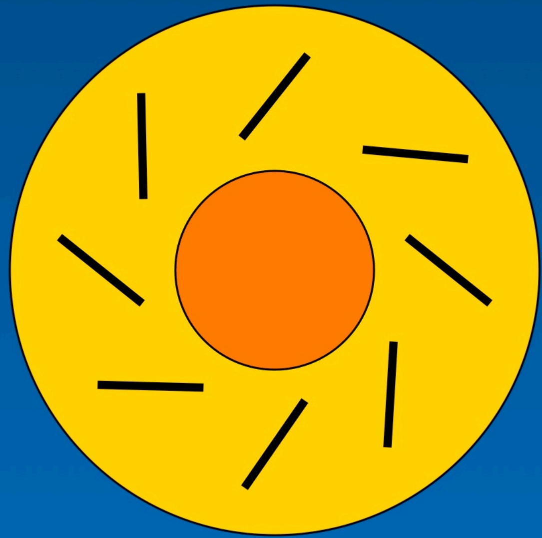

E Polarization

$$\nabla \times E = 0$$

B Polarization

$$\nabla \cdot B = 0$$

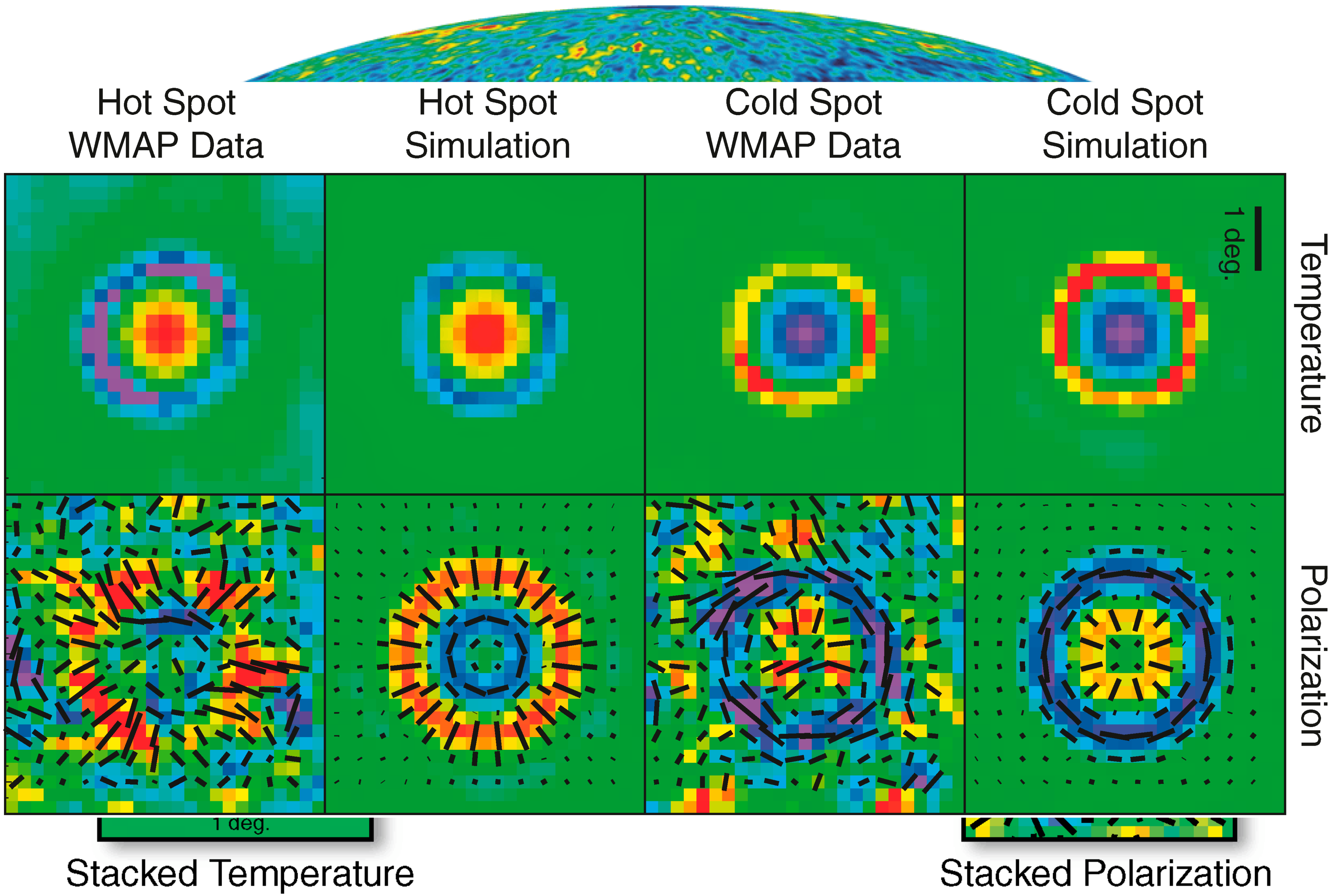
Hot Spot
WMAP Data
Hot Spot
Simulation
Cold Spot
WMAP Data
Cold Spot
Simulation
1 deg.
Temperature
Polarization
1 deg.
Stacked Temperature
Stacked Polarization

The CMB sky: spherical harmonics

$$T(\mathbf{n}) = \sum_{\ell m} a_{T,\ell m} Y_{\ell m}(\mathbf{n})$$

$$P_{\pm\pm}(\mathbf{n}) = (Q \pm iU)(\mathbf{n}) = \sum_{\ell m} a_{\pm 2,\ell m} \ {}_{\pm 2}Y_{\ell m}(\mathbf{n})$$

$${}_{\pm 2}Y_{\ell m}(\mathbf{n}) = 2\sqrt{\frac{(\ell-2)!}{(\ell+2)!}} \nabla_{\mathbf{e}_\pm} \nabla_{\mathbf{e}_\pm} Y_{\ell m}(\mathbf{n})$$

The non-local, rotationally invariant, spin-0 E- and B-modes

$$E(\mathbf{n}) = \sum_{\ell m} a_{E,\ell m} Y_{\ell m}(\mathbf{n}) \qquad a_{E,\ell m} \equiv \frac{-1}{2}(a_{2,\ell m} + a_{-2,\ell m})$$

$$B(\mathbf{n}) = \sum_{\ell m} a_{B,\ell m} Y_{\ell m}(\mathbf{n}) \qquad a_{E,\ell m} \equiv \frac{i}{2}(a_{2,\ell m} - a_{-2,\ell m})$$

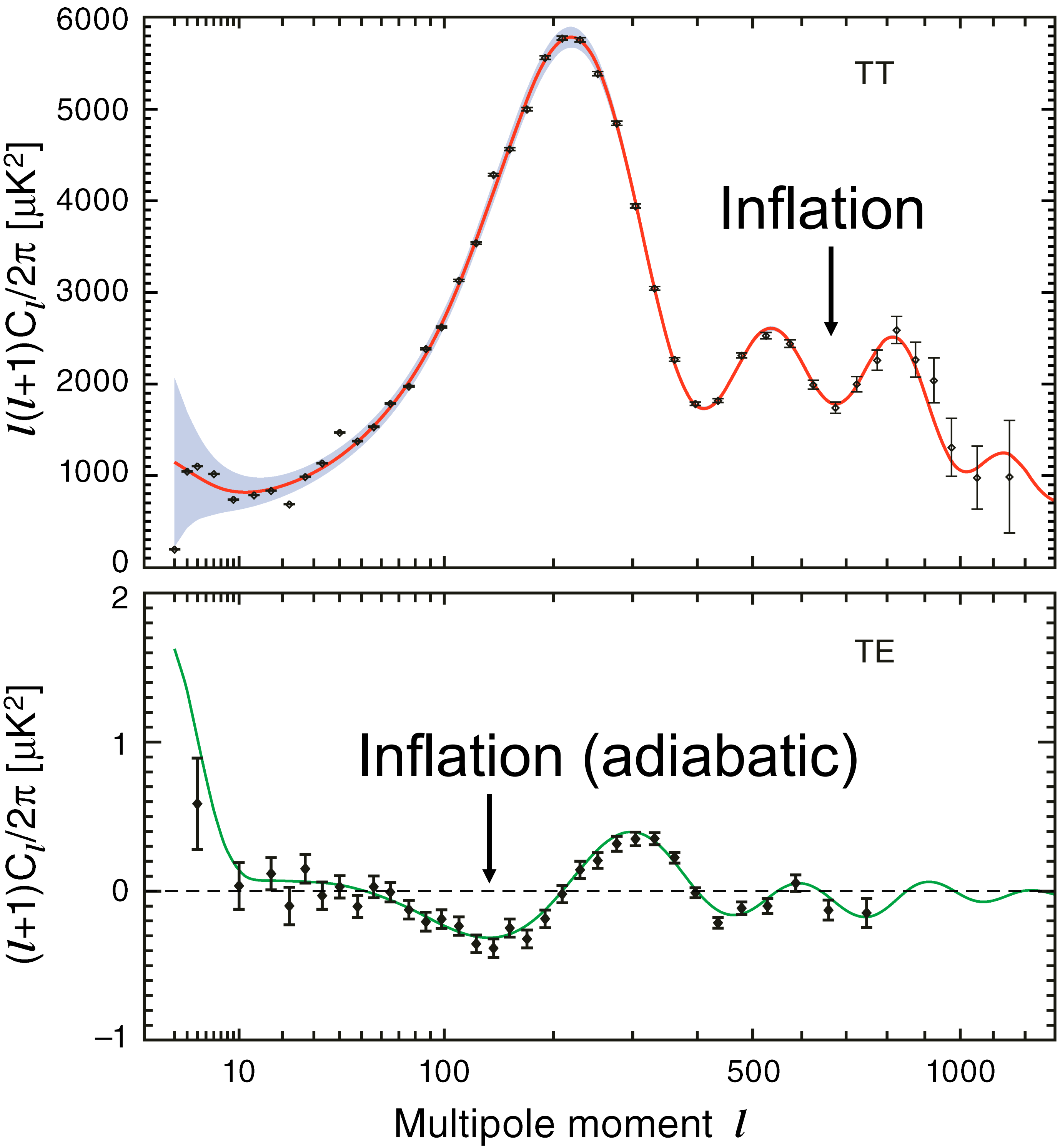
6000
5000
4000
3000
2000
1000
0
TT
Inflation
$l(l+1)C_l/2\pi$ [μK^2]
2
1
0
−1
TE
Inflation (adiabatic)
$(l+1)C_l/2\pi$ [μK^2]
10
100
500
1000
Multipole moment l

Non-local E- and B-modes

The relation between E and B-modes and the Stokes parameters Q and U in real space is *non-local.*

$$Y_{\ell m}(\mathbf{n}) \to \frac{1}{2\pi} e^{i\ell\cdot\mathbf{x}}$$

$\mathbf{x} = (x, y)$ orthogonal to the line of sight

$$E(\mathbf{x}) = \nabla^{-2}\left[\left(\partial_x^2 - \partial_y^2\right)Q(\mathbf{x}) + 2\,\partial_x\partial_y\,U(\mathbf{x})\right]$$

$$B(\mathbf{x}) = \nabla^{-2}\left[\left(\partial_x^2 - \partial_y^2\right)U(\mathbf{x}) - 2\,\partial_x\partial_y\,Q(\mathbf{x})\right]$$

Need to know (Q, U) *globally* in order to determine (E, B)

The *local* $(\tilde{E}, \tilde{B})$ modes are determined *locally* by (Q, U)

Local Ẽ- and B̃-modes

$$\nabla_- \nabla_- P_{++} + \nabla_+ \nabla_+ P_{--} = 2\nabla_a \nabla_b P_{ab} \equiv \tilde{E}\,,$$

$$\nabla_- \nabla_- P_{++} - \nabla_+ \nabla_+ P_{--} = 2\epsilon_{cd}\epsilon_{ab} \nabla_c \nabla_a P_{bd} \equiv \tilde{B}\,.$$

$$\tilde{E}(\mathbf{n}) = \sum_{\ell m} a_{\tilde{E},\ell m} Y_{\ell m}(\mathbf{n}) \qquad a_{\tilde{E},\ell m} \equiv \sqrt{n_\ell}\, a_{E,\ell m}$$

$$\tilde{B}(\mathbf{n}) = \sum_{\ell m} a_{\tilde{B},\ell m} Y_{\ell m}(\mathbf{n}) \qquad a_{\tilde{B},\ell m} \equiv \sqrt{n_\ell}\, a_{B,\ell m}$$

$$n_\ell = \frac{(\ell+2)!}{(\ell-2)!} = \ell(\ell^2-1)(\ell+2) \sim \ell^4$$

Power spectra and correlation functions

The rotationally-invariant angular power spectra

$$\langle a^*_{X,\ell m} a_{Y,\ell' m'} \rangle = C_\ell^{XY} \, \delta_{\ell\ell'} \delta_{mm'} \qquad X, Y = T, E, B$$

The real space angular correlation functions

$$C^{XY}(\theta) \equiv \langle X(\mathbf{n}) Y(\mathbf{n}') \rangle_{\mathbf{n}\cdot\mathbf{n}'=\cos\theta} = \sum_\ell \frac{2\ell+1}{4\pi} C_\ell^{XY} \, P_\ell(\cos\theta)$$

Also for local $\tilde{\text{B}}$-modes

$$C^{\tilde{B}}(\theta) \equiv \langle \tilde{B}(\mathbf{n}) \tilde{B}(\mathbf{n}') \rangle_{\mathbf{n}\cdot\mathbf{n}'=\cos\theta}$$

$$C^{\tilde{B}}(\theta) = \frac{1}{4\pi} \sum_{\ell=2}^{\infty} \frac{(\ell+2)!}{(\ell-2)!} (2\ell+1) P_\ell(\cos\theta) C_\ell^B$$

Contribution of defects to CMB polarization anisotropies

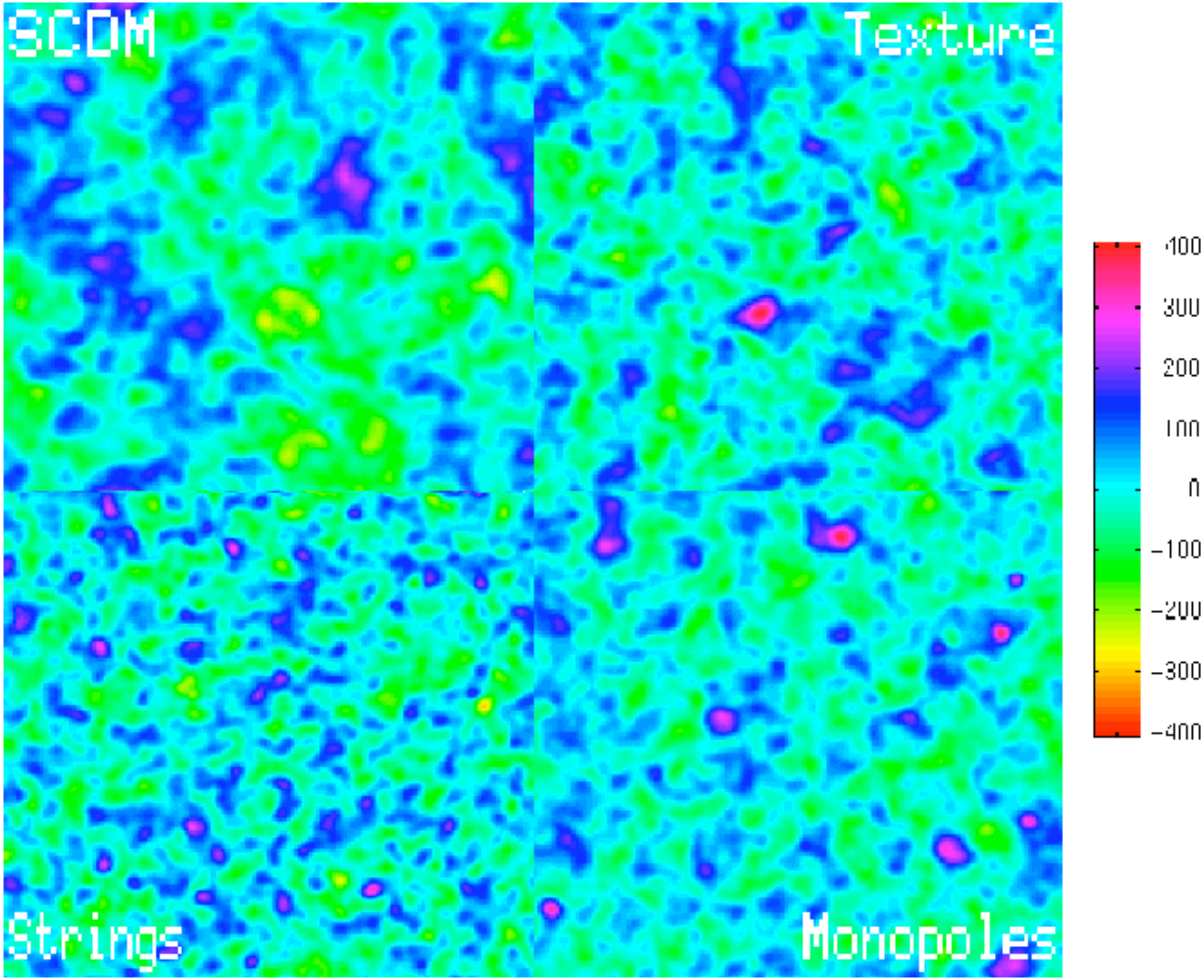
SCDM
Texture
Strings
Monopoles
400
300
200
100
0
−100
−200
−300
−400

Cosmic Strings components: S, V, T

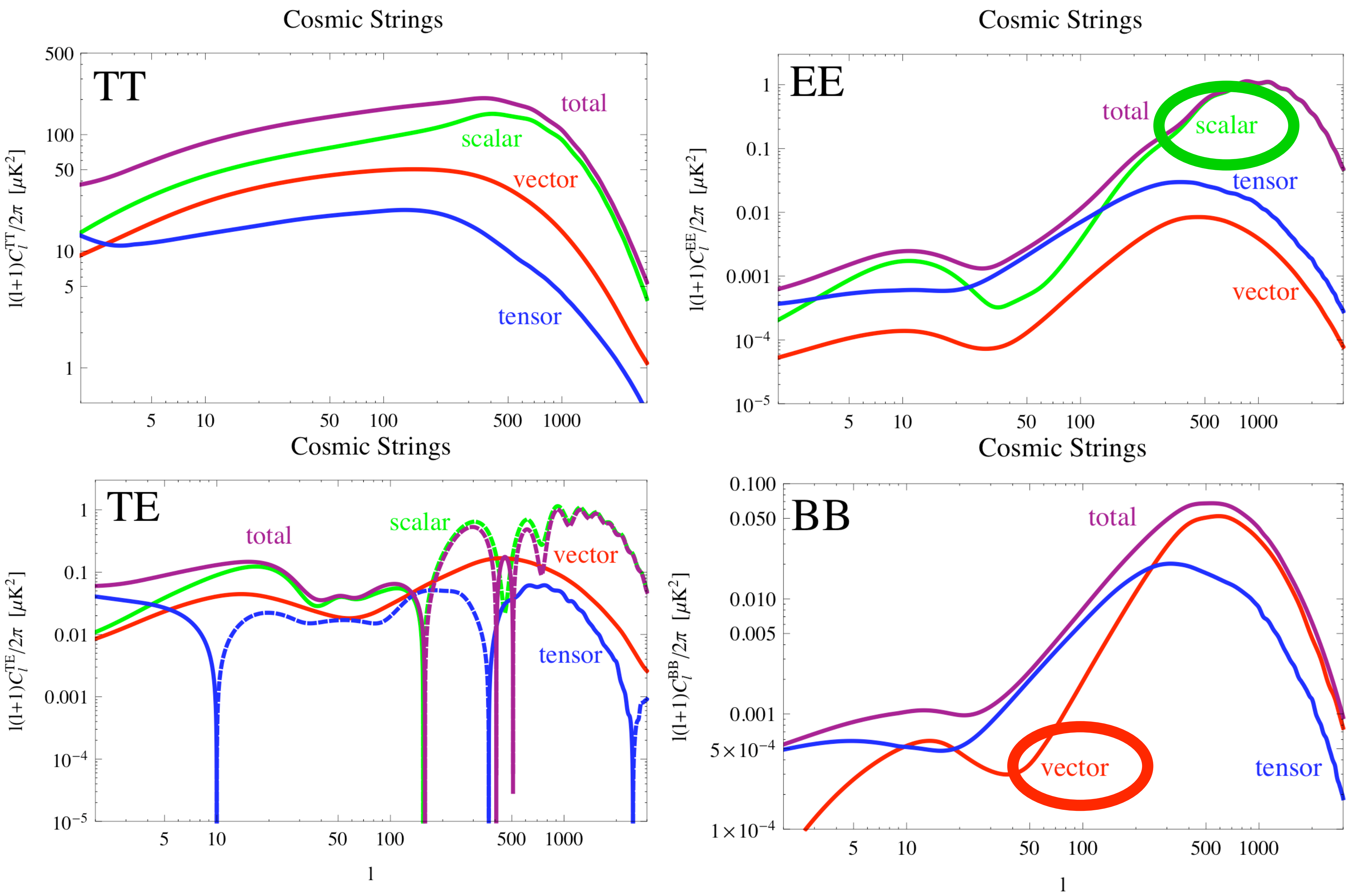

Angular power spectra Cosmic Strings

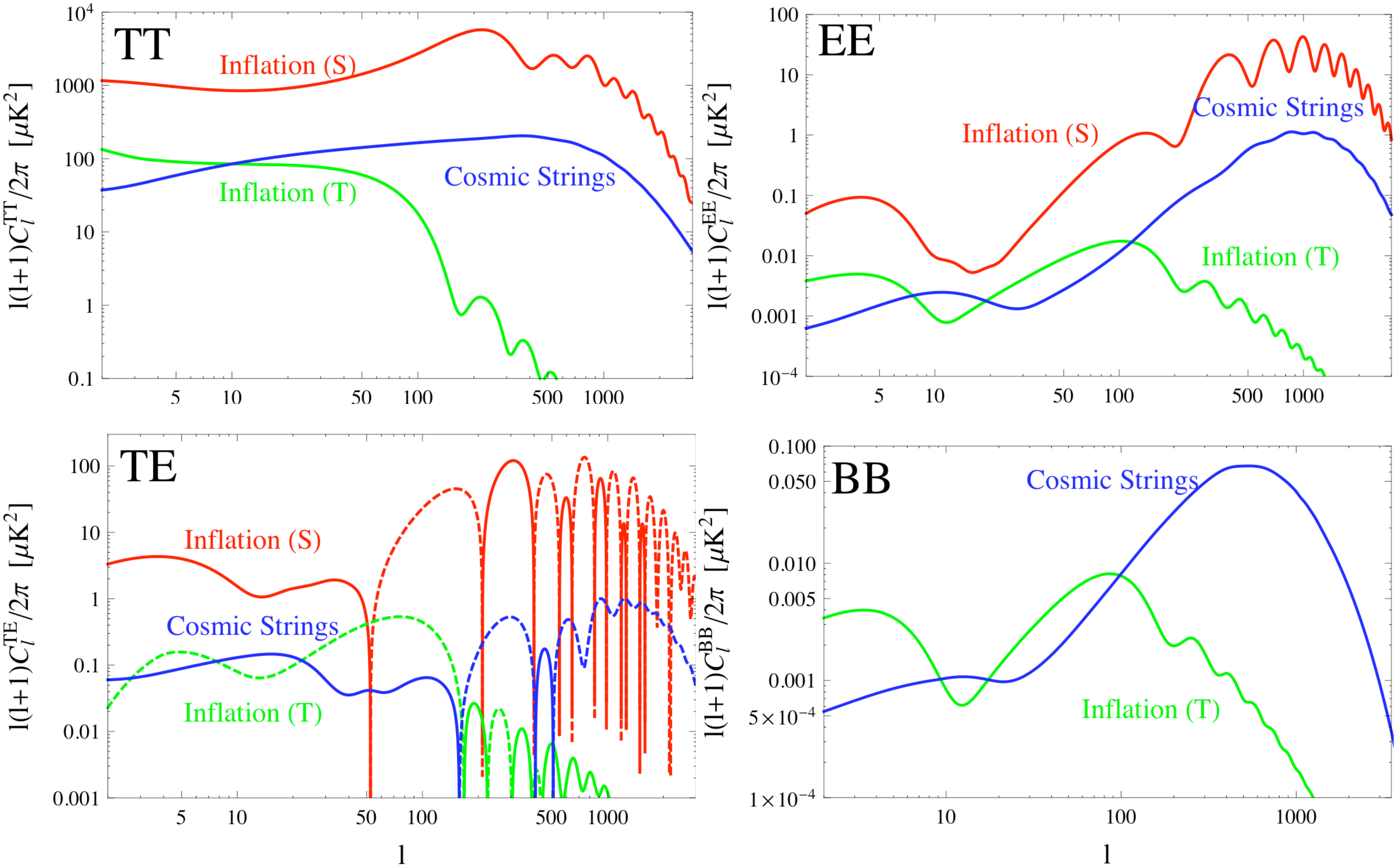

Real unbinned WMAP data (TT)

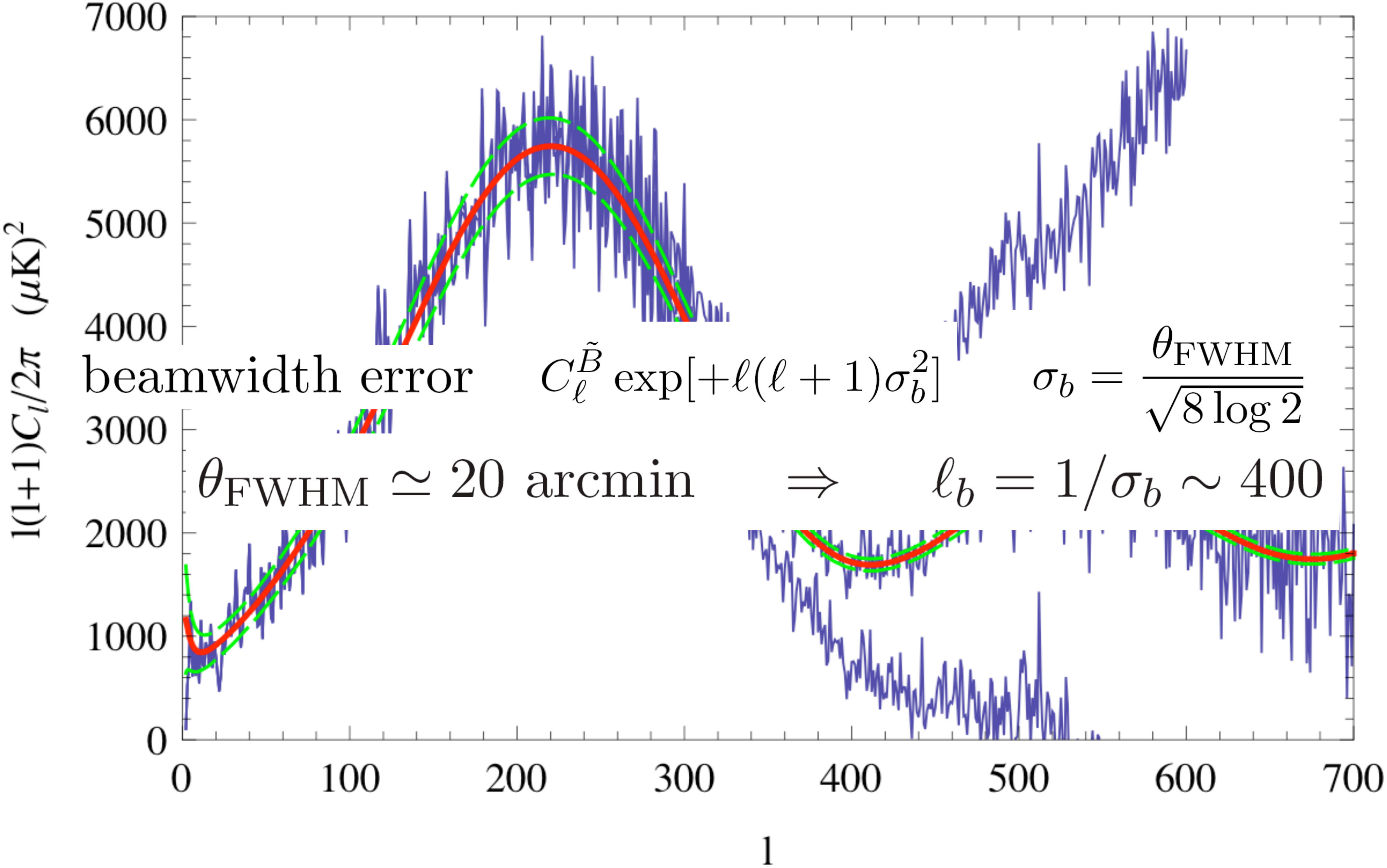

beamwidth error $C_\ell^{\tilde{B}} \exp[+\ell(\ell+1)\sigma_b^2]$ $\sigma_b = \frac{\theta_{\rm FWHM}}{\sqrt{8\log 2}}$

$\theta_{\rm FWHM} \simeq 20$ arcmin $\Rightarrow$ $\ell_b = 1/\sigma_b \sim 400$

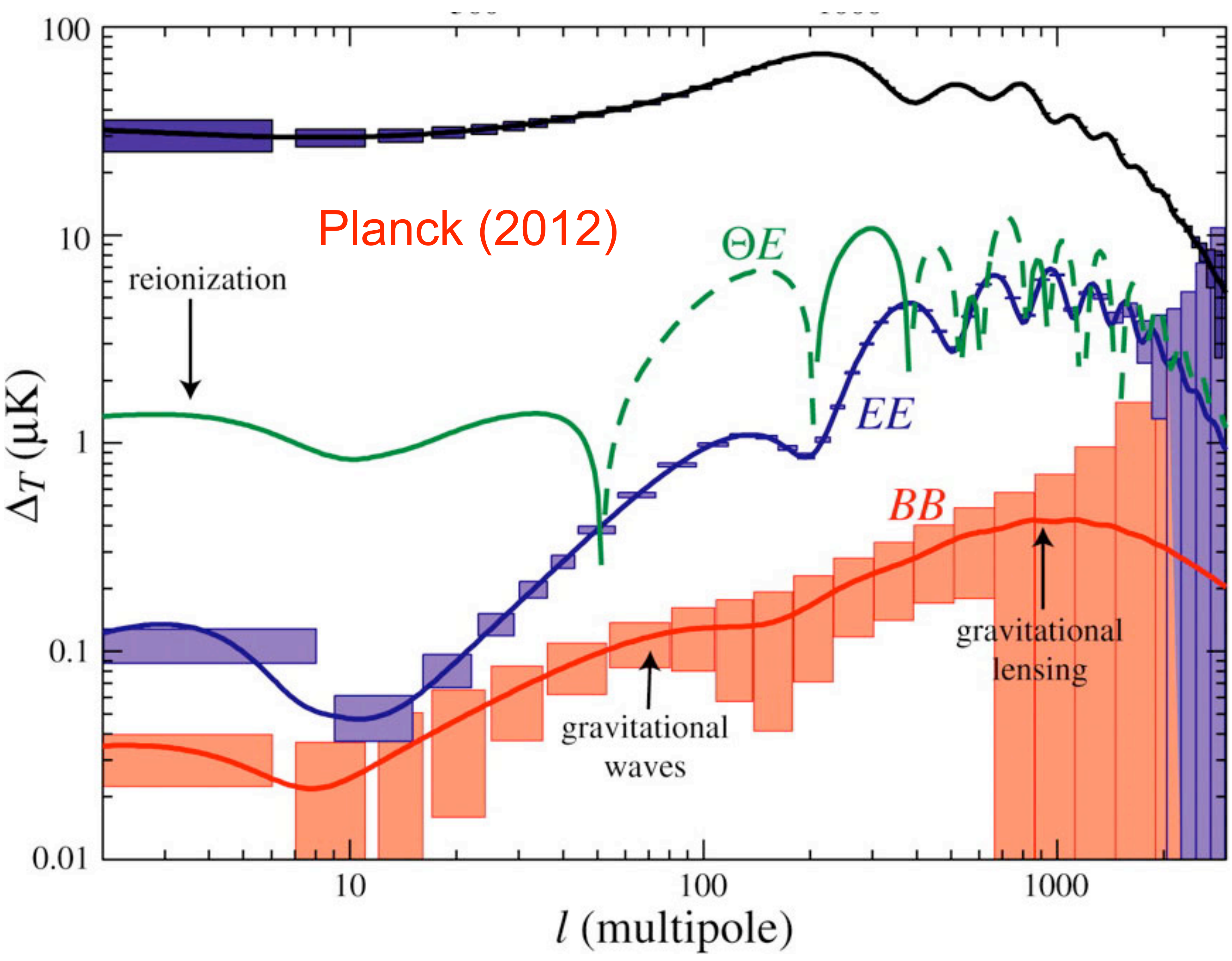

Planck (2012)
reionization
ΘE
EE
BB
gravitational waves
gravitational lensing
Δ_T (μK)
l (multipole)
100
10
1
0.1
0.01
10
100
1000

Lensing cleaning of B-modes

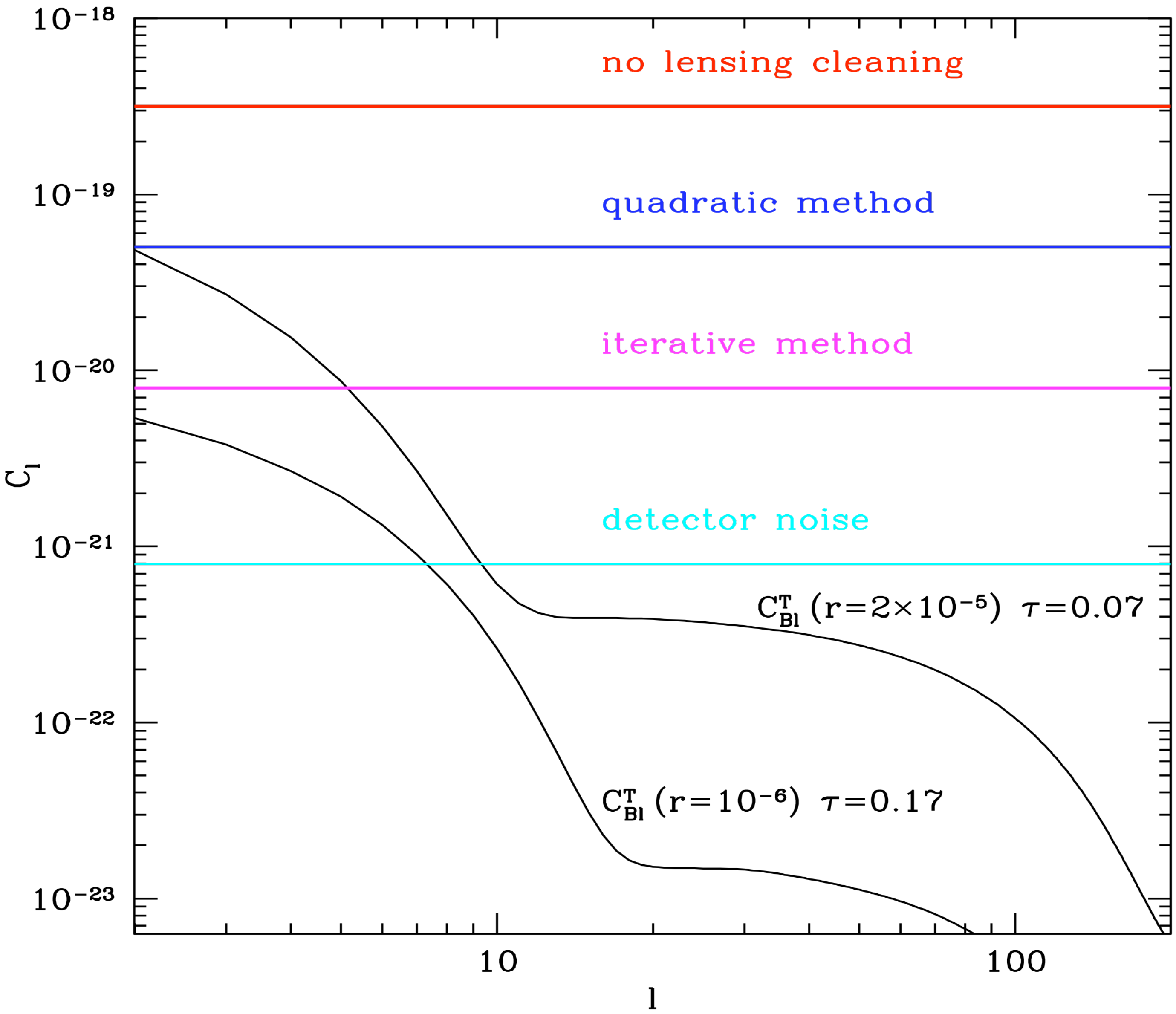

Gaussian smoothing

$N_\ell = \Delta_{P,\mathrm{eff}}\, n_\ell$ very blue noise power spectrum

$$\Delta_{P,\mathrm{eff}} = (0.5 - 12)\,\mu\mathrm{K}{\cdot}\mathrm{arcmin}$$

Planck
CMBpol

$$\mathcal{C}_\ell^{\tilde{B}} = (C_\ell^{\tilde{B}} + N_\ell)\exp[-\ell(\ell+1)/\ell_s^2]$$

Gaussian smoothing of width σ_s

corresponding to a smoothing scale $\ell_s < \ell_b \sim 800$

Angular Power Spectrum $\tilde{B}$-modes

JGB, Durrer, Fenu, Figueroa, Kunz arXiv:1003.0299

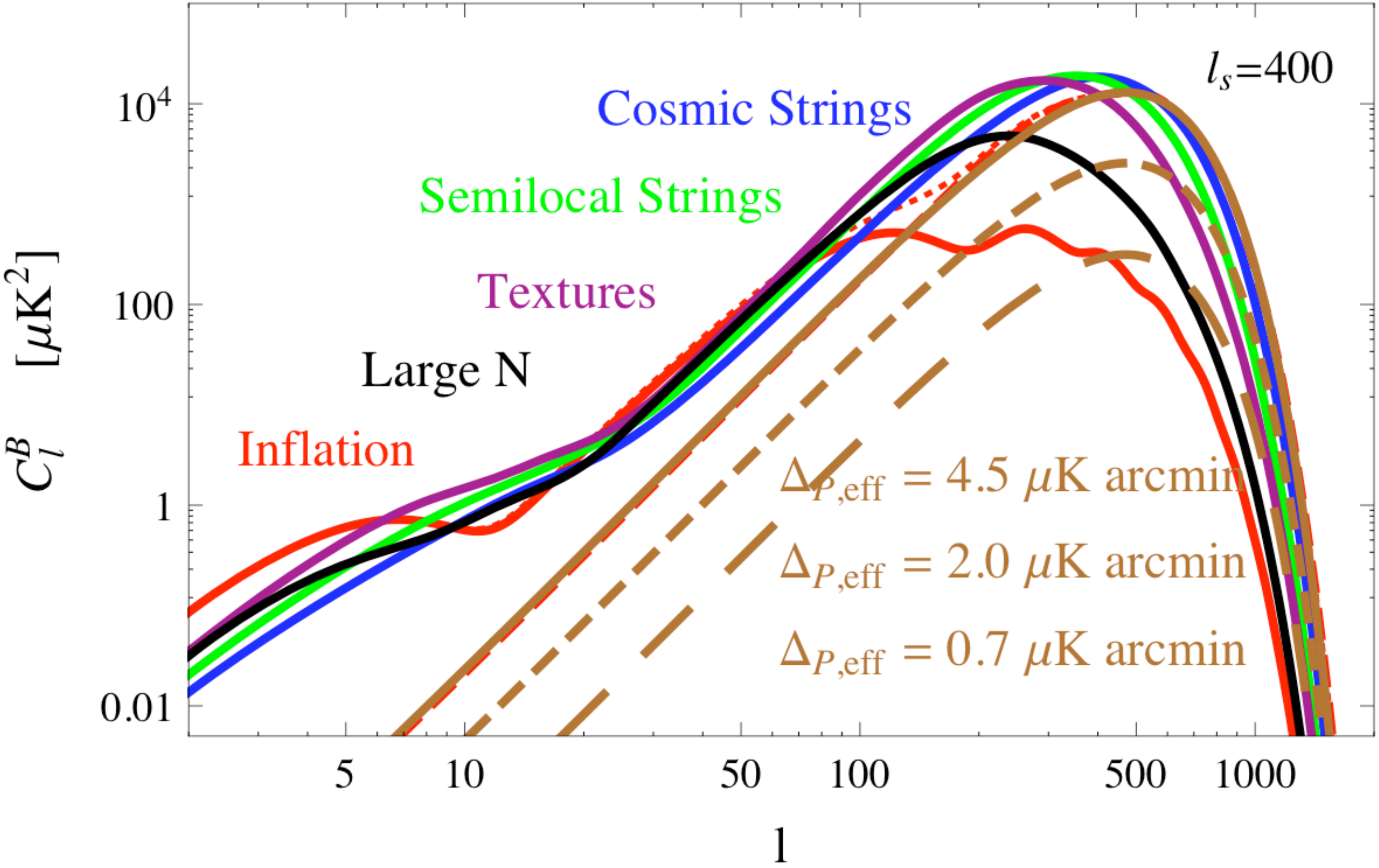

Correlation function with Noise

JGB, Durrer, Fenu, Figueroa, Kunz arXiv:1003.0299

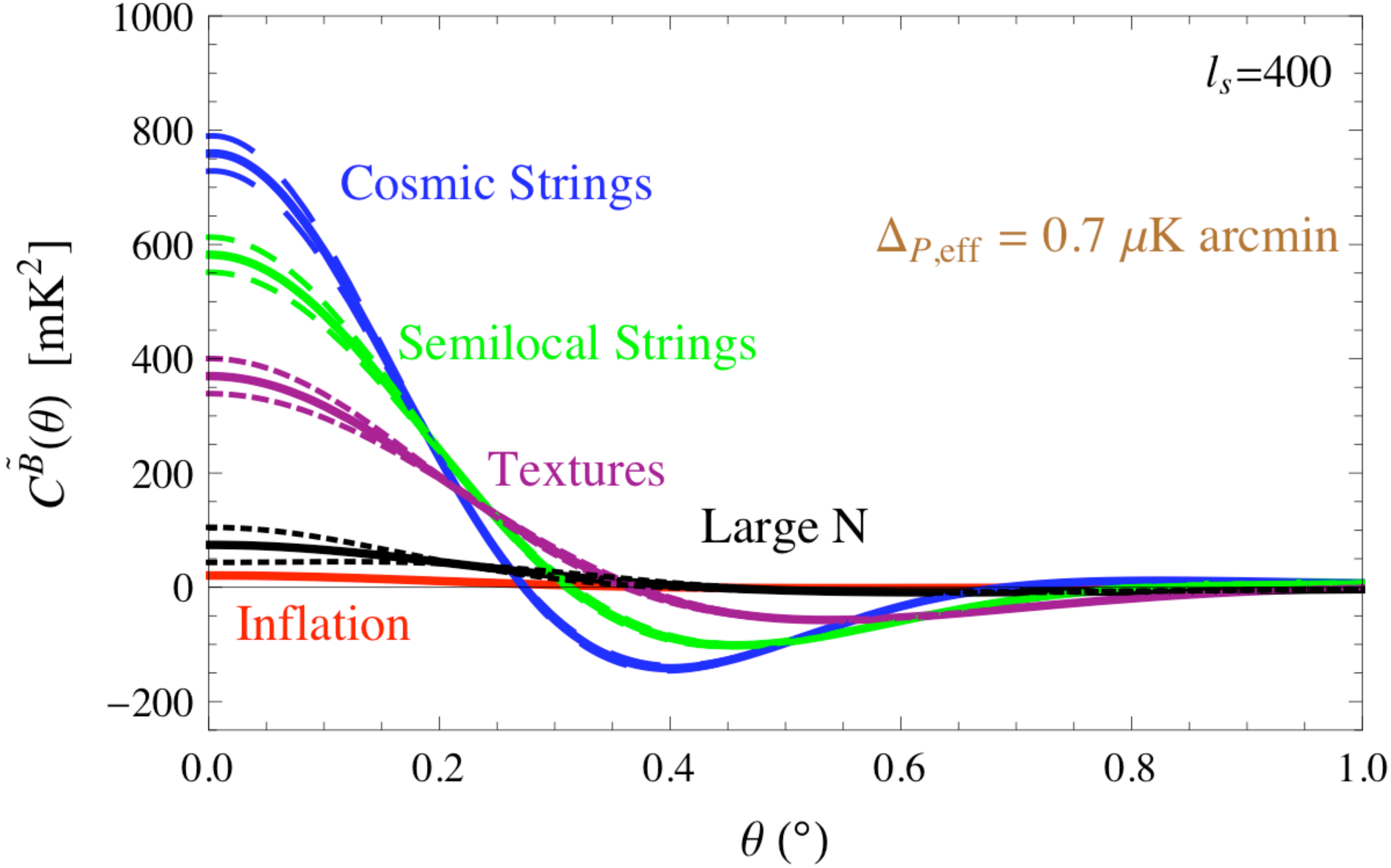

Angular correlation function B̃-modes

JGB, Durrer, Fenu, Figueroa, Kunz arXiv:1003.0299

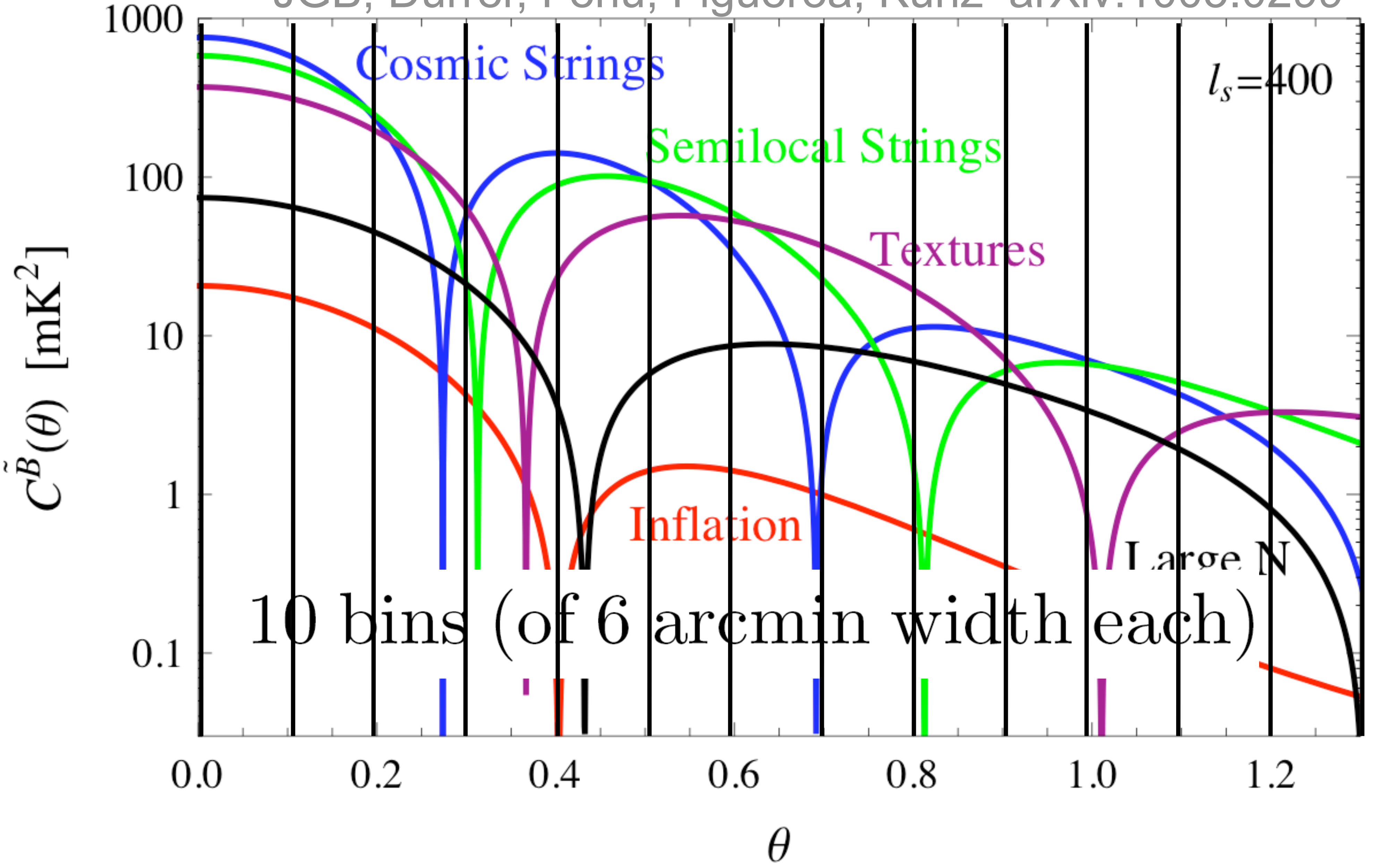

Signal to noise ratio (BB)

$$\mathsf{S}_i = C^{\tilde{B}}(\theta_i) \qquad \theta_i \,\epsilon\, [0, 1^o] \qquad S/N = \sqrt{\mathsf{S}_i \mathsf{C}_{ij}^{-1} \mathsf{S}_j}$$

$$\mathsf{C}_{ij} = \sum_{\ell} \frac{2\ell + 1}{8\pi^2 f_{\rm sky}} (\mathcal{C}_\ell^{\tilde{B}})^2 P_\ell(\cos\theta_i) P_\ell(\cos\theta_j)$$

covariance matrix in ℓ-space was assumed to be diagonal

$$\mathrm{cov}[\mathcal{C}_\ell^{\tilde{B}}, \mathcal{C}_{\ell'}^{\tilde{B}}] = \frac{2}{(2\ell + 1) f_{\rm sky}} (\mathcal{C}_\ell^{\tilde{B}})^2 \delta_{\ell\ell'}$$

Signal to Noise ratio for defects

JGB, Durrer, Fenu, Figueroa, Kunz arXiv:1003.0299

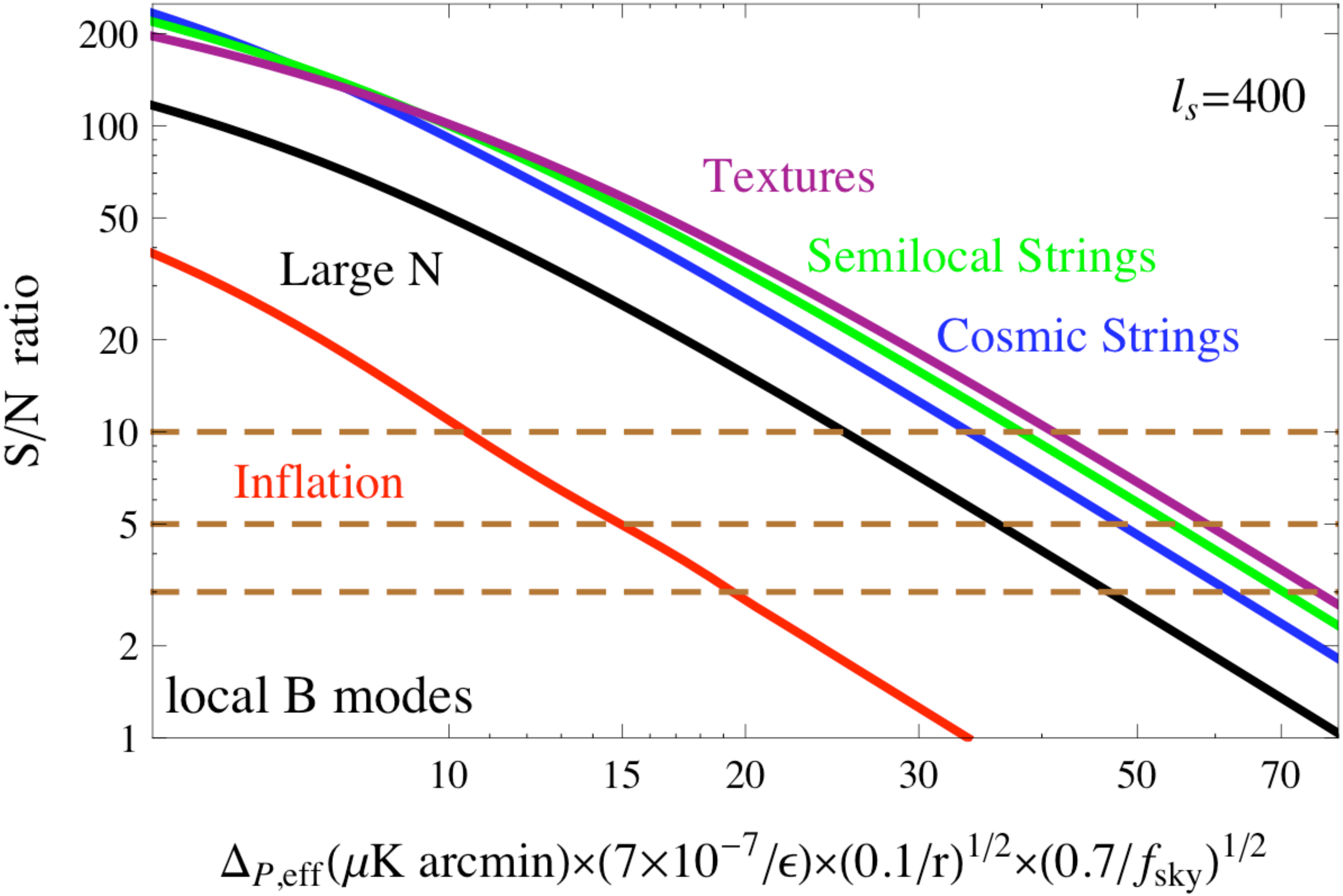

Comparison local vs non-local modes

JGB, Durrer, Fenu, Figueroa, Kunz arXiv:1003.0299

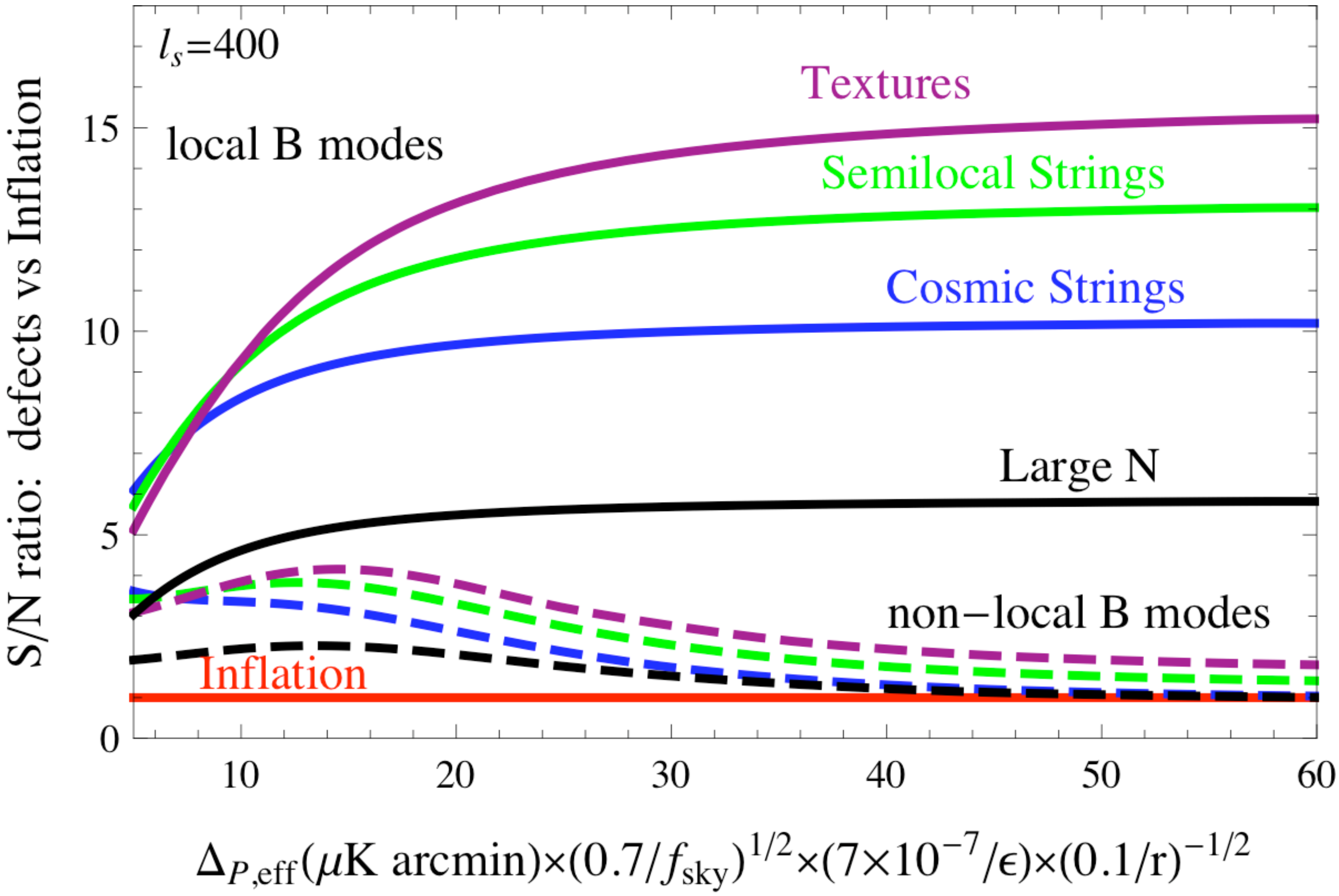

Limits on defects and inflation

$S/N = 3$	Inflation	Strings	Semilocal	Textures	Large-N
Planck	0.03	1.2×10^{-7}	1.1×10^{-7}	1.0×10^{-7}	1.6×10^{-7}
CMBpol	10^{-4}	7.7×10^{-9}	6.9×10^{-9}	6.3×10^{-9}	1.0×10^{-8}
$\tilde{B}$ exp	10^{-7}	1.1×10^{-10}	1.0×10^{-10}	0.9×10^{-10}	1.4×10^{-10}

Table 1: The limiting amplitude for inflation ($r = T/S$) and various defects ($\epsilon = Gv^2$), at 3-σ in the range $\theta \in [0, 1^o]$, for Planck ($\Delta_{P,\text{eff}} = 11.2\,\mu$K·arcmin), CMBpol-like exp. ($\Delta_{P,\text{eff}} = 0.7\,\mu$K·arcmin) and a dedicated CMB experiment with ($\Delta_{P,\text{eff}} = 0.01\,\mu$K·arcmin). We set $f_{\text{sky}} = 0.7$ in all of them.

Particle Physics connection

$$M_{\text{inf}} = 1.63 \times 10^{16}\ \text{GeV} \left(\frac{r}{0.1}\right)^{1/4} \qquad v = 1.02 \times 10^{16}\ \text{GeV} \left(\frac{\epsilon}{7 \times 10^{-7}}\right)^{1/2}$$

$S/N = 3$	Inflation	Strings	Semilocal	Textures	Large-N
Planck	1.2×10^{16}	4.2×10^{15}	4.0×10^{15}	3.9×10^{15}	4.9×10^{15}
CMBpol	2.9×10^{15}	1.1×10^{15}	1.0×10^{15}	9.7×10^{14}	1.2×10^{15}
$\tilde{B}$ exp	5.2×10^{14}	1.3×10^{14}	1.2×10^{14}	1.1×10^{14}	1.4×10^{14}

Conclusions

- Inflation produces scalar and tensor perturb.
- CMB anisotropies and LSS consistent with it
- Production of PGW at preheating (Big Bang)
- Different sources of GW during/after inflation
- Topological & non-top. defect prod. @ preh.
- Can distinguish between different sources
- Key observable: local B-modes
- Connection to high energy particle physics